



Drivers, dynamics and impacts of changing Arctic coasts

Anna M. Irrgang  ¹✉, Mette Bendixen  ², Louise M. Farquharson  ³, Alisa V. Baranskaya  ⁴, Li H. Erikson  ⁵, Ann E. Gibbs  ⁵, Stanislav A. Ogorodov  ⁴, Pier Paul Overduin  ¹, Hugues Lantuit  ^{1,6}, Mikhail N. Grigoriev  ⁷ and Benjamin M. Jones  ⁸

Abstract | Arctic coasts are vulnerable to the effects of climate change, including rising sea levels and the loss of permafrost, sea ice and glaciers. Assessing the influence of anthropogenic warming on Arctic coastal dynamics, however, is challenged by the limited availability of observational, oceanographic and environmental data. Yet, with the majority of permafrost coasts being erosive, coupled with projected intensification of erosion and flooding, understanding these changes is critical. In this Review, we describe the morphological diversity of Arctic coasts, discuss important drivers of coastal change, explain the specific sensitivity of Arctic coasts to climate change and provide an overview of pan-Arctic shoreline change and its multifaceted impacts. Arctic coastal changes impact the human environment by threatening coastal settlements, infrastructure, cultural sites and archaeological remains. Changing sediment fluxes also impact the natural environment through carbon, nutrient and pollutant release on a magnitude that remains difficult to predict. Increasing transdisciplinary and interdisciplinary collaboration efforts will build the foundation for identifying sustainable solutions and adaptation strategies to reduce future risks for those living on, working at and visiting the rapidly changing Arctic coast.

¹Alfred Wegener Institute Helmholtz Centre for Polar and Marine Research, Potsdam, Germany.

²Department of Geography, McGill University, Montreal, Canada.

³Geophysical Institute, University of Alaska Fairbanks, Fairbanks, AK, USA.

⁴Lomonosov Moscow State University, Moscow, Russia.

⁵US Geological Survey, Pacific Coastal and Marine Science Center, Santa Cruz, CA, USA.

⁶Institute of Geosciences, University of Potsdam, Potsdam, Germany.

⁷Melnikov Permafrost Institute, Yakutsk, Russia.

⁸Institute of Northern Engineering, University of Alaska Fairbanks, Fairbanks, AK, USA.

✉e-mail: anna.irrgang@awi.de
<https://doi.org/10.1038/s43017-021-00232-1>

Arctic coasts are influenced by the presence of sea ice, permafrost and ground ice^{1–3}. The presence of ice onshore and offshore makes Arctic coasts particularly sensitive to the effects of climate warming. The most visible changes are to shoreline position, predominantly by shoreline retreat through erosion^{4,5}. To a lesser extent, shoreline progradation through accumulation also shapes Arctic coasts^{4,5}. The interplay and combined effects of oceanographic, terrestrial, periglacial and paraglacial processes lead to changes in shoreline position and cause the redistribution of sediments, carbon, nutrients and contaminants within the coastal zone and into the offshore marine environment^{6–8}.

Permafrost coasts are particularly vulnerable to rising air temperatures; warm air acts upon the soil column from the top down and laterally inwards from the bluff face. This combination leads to rapid ground-ice melt and permafrost thaw, making the coast more susceptible to erosion^{2,9}. Climate warming is amplified in the Arctic. For example, between 1971 and 2017, Arctic surface air temperatures rose 2.4 times faster than the Northern Hemisphere average¹⁰, with mean annual, cold season and warm season Arctic air temperatures increasing by 2.7°C, 3.1°C and 1.8°C, respectively¹⁰. Furthermore, 9 of the years between 2010 and 2020, recorded average surface air temperature anomalies of more than 1°C, making

them the warmest years since 1900 (REF.¹¹). In the same time period, numerous sites along permafrost coasts recorded an increase of erosion rates⁴.

Rising air temperature also influences the extent and spatiotemporal distribution of sea ice. The ten lowest sea-ice extents since the beginning of satellite-based observations in 1979 were recorded between 2010 and 2021, with the exception of 2014 (REF.¹²). Consequently, the effects of climate-change-induced stressors on the terrestrial and marine environments are leading to more rapid landscape and coastal morphological changes along Arctic coasts, compared with historical rates of change^{13,14}, however, for much of the Arctic, only limited data exist.

In 1999, the Arctic Coastal Dynamics project was launched as an initiative of the International Permafrost Association and the International Arctic Science Committee to provide an international platform for Arctic coastal researchers. The release of the Arctic Coastal Dynamics (ACD) database¹⁵ and corresponding publication⁵ in 2011 marked a turning point in Arctic coastal research. The ACD database contains a pan-Arctic assessment of shoreline change rates, backshore elevation and coastal ground-ice distribution. Entries largely rely on expert estimates and, currently, this is the only dataset that allows for a pan-Arctic

Key points

- Arctic coasts are some of the most rapidly changing coasts on Earth. Most change occurs during the sea-ice-free period, which can be up to 3 months.
- The erosion of permafrost coasts has increased since the early 2000s when compared with the late twentieth century (1960s–1990s), coinciding with an intensification of environmental drivers linked to anthropogenic warming.
- Mean annual erosion rates along stretches of unlithified permafrost coasts in Alaska, Canada and Siberia have more than doubled since the early 2000s compared with the latter half of the twentieth century.
- Coastal erosion along permafrost coasts is expected to continue at high rates or even accelerate in response to further climate warming.
- Rapid environmental and social change in the Arctic highlights the need for coordinated interdisciplinary and transdisciplinary efforts of scientists, stakeholders and policymakers, together with the local coastal population, to develop adaptive strategies around Arctic coasts in transition.

Permafrost

Subsurface materials that remain continuously at or below 0 °C for at least 2 consecutive years.

Shoreline progradation

Seaward advance of the shoreline.

Periglacial

Processes influenced by intense freeze–thaw and/or permafrost.

Paraglacial

Non-glacial geomorphological processes conditioned by glaciation.

Bluff face

Sea-facing slope between bluff toe and bluff top.

Coastal dynamics

The ongoing transition of coastal processes caused by the interplay and combined effects of oceanographic, terrestrial, periglacial and paraglacial processes, and the resulting redistribution of sediment, carbon, nutrients and contaminants.

Unlithified

Composed of sediment clasts, not bedrock.

Lithified

The transformation and cementation of sediments into solid rock (singular, lithic).

Syngenetic

Ground-ice formation occurring in synchrony with sediment accumulation.

Epigenetic

Ice formation occurring post-deposition (in contrast to syngenetic).

comparison of shoreline change rates. Further development of the ACD database will help in understanding how climate warming influences Arctic coastal dynamics.

To date, only a very limited number of reviews have focused on Arctic coastal dynamics^{16,17}. Past reviews primarily addressed differences in geomorphology among Arctic coasts and the evolution of rates of shoreline change^{16,17}. Notably, the State of the Arctic coast 2010 report provided a comprehensive integration of physical, ecological and socio-economical aspects related to coastal change, and explored factors that influence the capability of Arctic coastal communities to respond to coastal changes¹⁸. However, since 2010, the lowest sea-ice extents and warmest air temperatures on record within the Arctic have been observed¹⁹. In addition, considerable research has been conducted to better understand how Arctic coastal dynamics have changed over the past two decades⁴ and what implications arise from these changes to the natural and human environment²⁰.

In this Review, we illustrate how the morphologic diversity and evolution of Arctic coasts describe the interplay between environmental drivers and the local coastal setting, and discuss how both are changing as an effect of a warming climate. We provide an overview of shoreline change evolution, with a particular focus on research developments since the early 2000s, and lay out the multifarious impacts that coastal dynamics have on the natural and built environment in the Arctic. We end by pointing out the relevance of Arctic coastal dynamics research, identify critical knowledge and data gaps that persist and provide suggestions for the future direction of Arctic coastal research. Unless otherwise stated, we focus on permafrost-affected coasts (FIG. 1) that border the Arctic Ocean, Greenland Sea, Baffin Bay and northern Hudson Bay. Throughout, the term coastal dynamics refers to the ongoing transition of the coast; the interplay and combined effects of oceanographic and terrestrial processes on the coast; and the resulting redistribution of sediment, carbon, nutrients and contaminants within the coastal zone and into the marine environment.

Geodiversity of Arctic coasts

Legacy effects of past glacial extent, Holocene landscape evolution and fluctuations in Pleistocene and Holocene sea level contribute to the modern-day geomorphology.

In addition, permafrost and ground-ice distributions characterize the Arctic coastal system¹⁷. These cryolithological and sedimentological properties, in turn, influence how environmental variables such as the sea-ice regime, sediment supply, hydrodynamics and temperature shape coastal dynamics^{21–24}.

Lithified and unlithified coasts. Arctic coasts are characterized by high geomorphic variability (FIG. 1) and encompass unlithified and lithified coasts, as well as permafrost-affected and non-permafrost-affected coasts (FIG. 2). Approximately 65% of the Arctic coasts are unlithified and 35% are lithic¹⁷. Unlithified but ice-bonded coasts primarily occur in Alaska, Canada and Siberia, and are characterized by ice-rich permafrost bluffs that range in height up to 40 m (REFS^{5,13,24–29}) (FIG. 1d,e), and lagoon–barrier island systems, beach ridge complexes, spits and deltas (FIG. 1a,b). By contrast, lithified coasts are characterized by a mix of low-lying rocky shorelines, fjords, bluffs and pocket beaches¹⁷ (FIG. 1c). Along lithified coasts, erosion is primarily driven by weathering in the form of freeze–thaw and wetting–drying cycles, combined with mechanical erosion from waves³⁰.

Ground-ice characteristics. The volume and distribution of ground ice contained in permafrost influences geomorphological processes, including the effectiveness of thermal and mechanical erosion³¹. Regional patterns of ground-ice distribution and volume are determined by Pleistocene and Holocene landscape dynamics and glacial history^{32–34}. Areas that remained unglaciated during the mid-Pleistocene to Late Pleistocene were exposed to aeolian, fluvial and marine depositional processes^{13,35–37} and a mix of syngenetic and epigenetic ground-ice accumulation^{32,38}, such as extensive regions of Siberia and northern Alaska. Unlithified, glaciated permafrost coasts can contain buried glacial ice and segregated ice within moraine deposits associated with the Laurentide and Fennoscandian ice sheets^{39–41}.

Unlithified coasts, such as those in Greenland, Svalbard and the Canadian Archipelago, tend to be unaffected by permafrost and contain little to no ground ice but, instead, large volumes of coarse, glacially derived sediment^{42–44}. Within such permafrost-free, unlithified systems, coastal processes are dominated by mechanical erosion and rapid sediment accumulation. If permafrost is found in such regions, it is usually poorly developed, dissected by taliks and prone to degradation due to saltwater intrusion⁴⁵. Ongoing glacial retreat from Little Ice Age advances has created a system out of geomorphological equilibrium that is in constant flux with high sediment transport rates and reworking^{42,46,47}. Dynamic landforms that characterize these coasts include barrier islands, spits, beach ridges, low-lying bluffs and prograding deltas, often with thin and sporadically distributed permafrost⁴⁸.

Emergent coasts are characterized by raised beach sequences⁴⁴ and heaved bedrock in regions experiencing ongoing isostatic uplift and, thus, relative sea-level fall, where permafrost aggradation can also occur if air temperatures allow^{49,50} (FIG. 1b). In some cases, ice-rich permafrost aggradation can also occur sub-aquatically

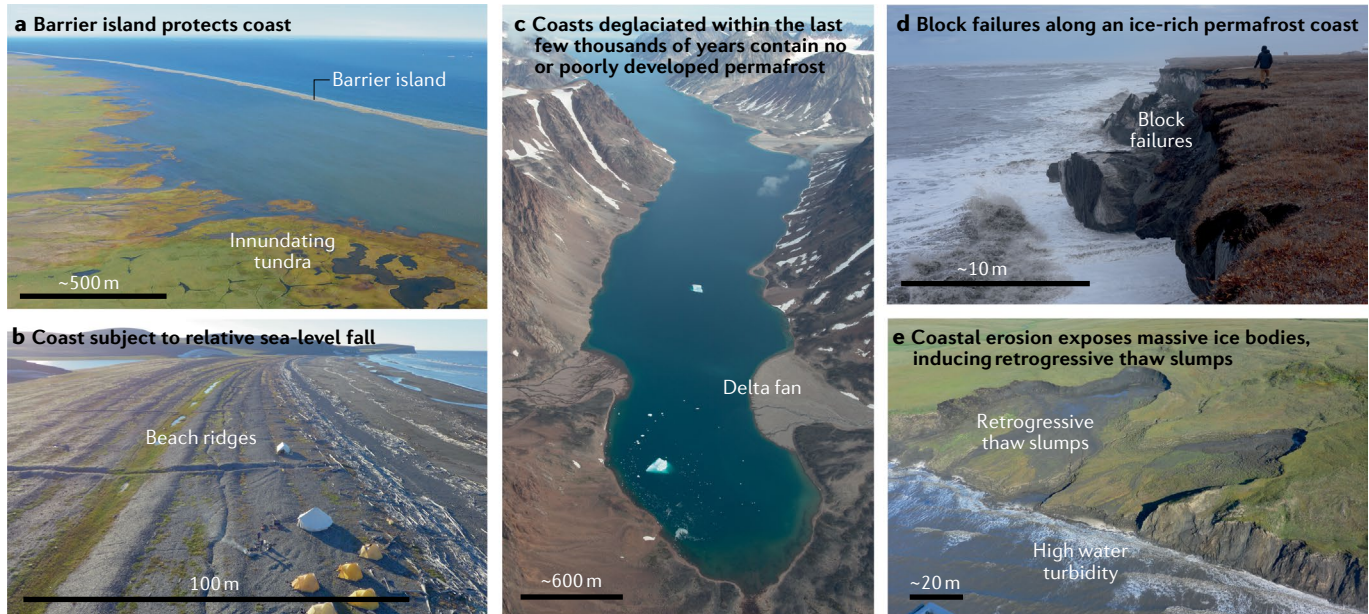


Fig. 1 | Examples of different Arctic coastal landforms. Arctic coasts have a high geomorphologic diversity, the overwhelming majority containing permafrost. **a** | Permafrost coast characterized by subsiding tundra protected by a barrier island (Canadian Beaufort coast). **b** | Paraglacial coast characterized by beach ridges (Buor Khaya Bay, Siberian Arctic). **c** | Fjord system with prograding delta fans (East Greenlandic coast). **d** | Ice-rich, permafrost-affected coast characterized by block failures (Alaskan Beaufort coast). **e** | Ice-rich permafrost coast characterized by a retrogressive thaw slump (Canadian Beaufort coast). Panel **b**, image courtesy of L. Sander. Panel **c**, image courtesy of A. A. Bjørk. Panel **e** adapted from REF.¹⁵², CC BY 4.0 (<https://creativecommons.org/licenses/by/4.0/>).

through talik refreeze, after a thermokarst lake transforms into a lagoon due to coastal erosion⁵¹. By contrast, coastal erosion and coastal flooding can degrade subsea permafrost and thaw ice-bonded sediments due to the transition from a cold terrestrial to a warmer marine environment⁵². Repeated sea-level highstands during the Pleistocene and early Holocene also led to the formation of saline marine deposits that contain cryopegs^{53,54}.

Arctic coasts are characterized by high geomorphic variability and consist of both unlithified and lithified material, and of permafrost-affected and non-permafrost-affected ground. The extent and distribution of permafrost and ground ice vary throughout the coast and, together with the coast's exposure to waves, are the most important local coastal characteristics that determine the nature and pace of coastal change processes.

Taliks

Ground in permafrost areas that remains unfrozen year round.

Thermokarst

Processes and landforms that result from the collapse of the land surface due to the melting of ground ice.

Cryopegs

A form of talik that remains unfrozen at temperatures below 0 °C due to the presence of saline water (brines).

Active layer

Layer on top of permafrost that is subject to annual summer thaw and winter freeze.

temperature⁵⁷, sea-ice dynamics and properties^{22,58}, wave climatology⁵⁹, storm intensity and timing^{60,61}, and sea-level changes⁶². Changes in the coastal setting and environmental drivers induce changes in the whole coastal system, although the complex interplay between the regional setting and environmental drivers, which includes geomorphological thresholds, lag times, feedback processes and mitigating factors, makes it difficult to split and directly correlate the influence that different components have on coastal dynamics.

Lithology and permafrost characteristics. Sedimentology and ice content and distribution exert an important control over the resistance of unlithified coasts to erosion¹⁷. Sediment composition determines the density of the sediments and their resistance to erosion⁶³; for example, dense clays generally have a lower erodibility compared with loams or sands. In turn, ground-ice distribution determines the potential for thermal denudation and the effectiveness of mechanical abrasion.

Ice-rich permafrost bluffs can be somewhat resistant to mechanical wave action and are comparable with lithified bluffs under freezing temperature conditions. However, if ice-rich permafrost bluffs are subject to thawing due to elevated air or water temperature, their erodibility increases considerably^{2,25}. Ground ice can be present in ice lenses, layers, massive ice beds and wide vertical ice veins, called ice wedges⁶⁴. In some areas, for example eastern Siberia or along the eastern Yukon coast in Canada, the ground-ice content of bluffs can reach over 90% with only small inclusions of sediment^{6,33}. When such ice-rich bluffs thaw, minimal sediment is left

and what remains is rapidly removed by wave action. For these combined reasons, unlithified coasts with high volumes of ground ice tend to retreat faster than coasts with less ground ice² (FIG. 3).

Air temperature. Air temperature is an important environmental driver of coastal change. It contributes greatly to processes that control coastal dynamics in the Arctic, including ground temperature and active layer thickness,

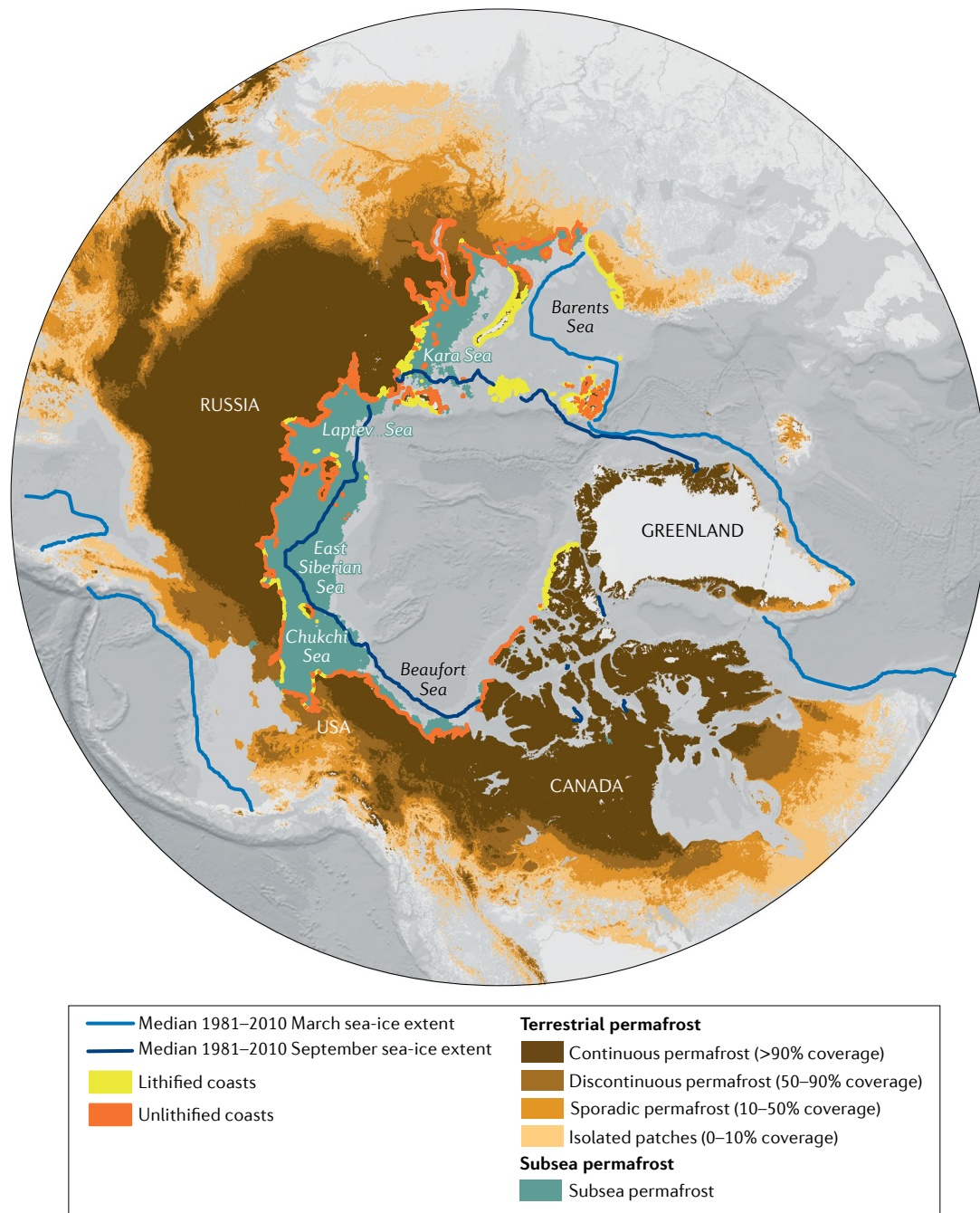


Fig. 2 | Map of Arctic coastal type, permafrost distribution and sea-ice extent. The pan-Arctic distribution of lithified and unlithified coasts¹⁵, terrestrial permafrost¹⁸¹, subsea permafrost¹⁸² and average maximum and minimum sea-ice extent¹². Most of the Arctic coast is affected by permafrost, and 65% is composed of unlithified but ice-bonded material⁵, which makes it particularly susceptible to the impacts of climate warming (lithification information is plotted only where data exist in the Arctic Coastal Dynamics database)¹⁵. Subsea permafrost is present along the Canadian, US and Russian coastal margins. The degradation of subsea permafrost in the nearshore zone leads to a lowering of the nearshore profile, allowing the transmission of more wave energy onshore. However, this process is considered to have a minor role for coastal erosion¹⁰⁷. Historically, maximum and minimum sea-ice extents, depicted with the 1981–2010 median March and September sea-ice limits¹², illustrate the great spatial variation in seasonal sea-ice cover. Where sea ice is absent during the summer, the coast is subject to wave action, which is most effective along unlithified coasts and contributes to coastal erosion²².

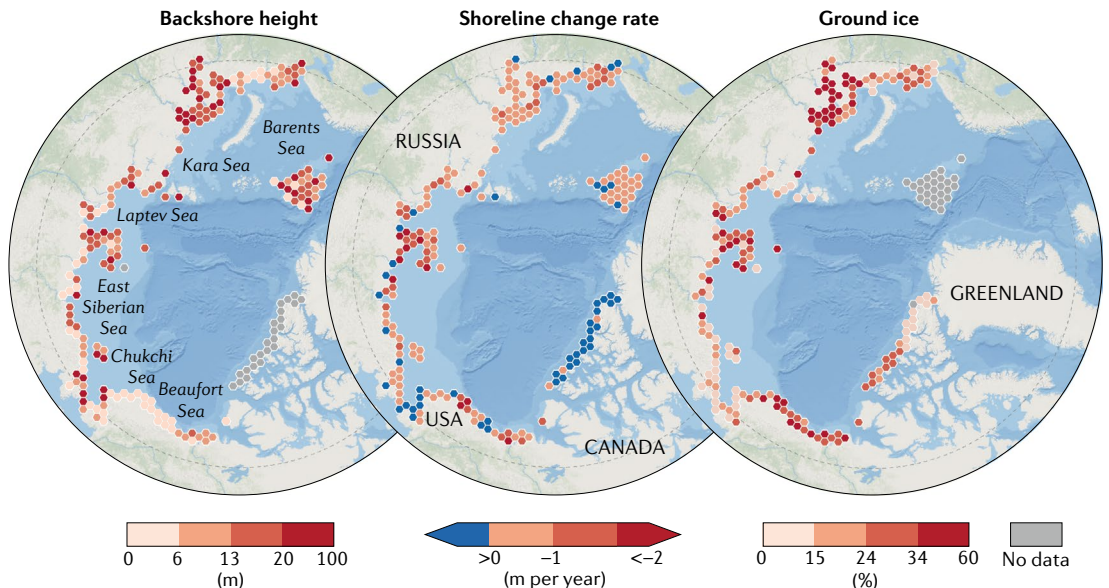


Fig. 3 | Variability of backshore height, ground-ice content and shoreline change rates along the Arctic coast. Data are from the Arctic Coastal Dynamics database¹⁵, summarized over a 100-km extent. Where no hexagons exist, such as along the coast of Greenland and Nowaja Semlja, Russia, no information is available in the Arctic Coastal Dynamics database. Note that unlithified permafrost coasts characterized by low bluffs and a high ice content, for example along the Laptev coast and the Beaufort coast, erode most rapidly. Despite partly high ground-ice content, lowest coastal change rates can be found along the Canadian Archipelago, which is subject to relative sea-level fall due to postglacial rebound¹³³.

sea temperature, sea-ice extent and the duration of sea-ice coverage. Especially along ice-rich permafrost bluffs, air temperature is an effective erosive agent, since, together with solar radiation, it governs the process of thermal denudation^{24,25,65,66}. Warm air and solar radiation cause the exposed ground ice in the bluff face to melt or ablate and previously ice-bonded sediments lose cohesion and move down the bluff face, from where they can be moved offshore by waves and wave-driven currents⁶⁷.

Thermal denudation has been observed to trigger erosion of the bluff top along ice-rich coasts, for example in the Laptev and Kara seas where wave action is absent^{24,25}. Further, increasing air temperatures during the summer lead to rising ground temperatures, active layer development and permafrost degradation, which leads to active layer detachments and thaw-induced subsidence of the coast, allowing for saltwater intrusion and accelerated erosion^{2,66}. While the individual effect of active layer depth on coastal erosion has not been constrained, on the Tuktoyaktuk coast in north-west Canada, it has been found that ground subsidence due to permafrost thaw led to volumetric land loss values three times higher than those directly associated with coastal erosion². Along glaciated coasts, air temperature can be the primary driver of shoreline change, because glacial melt governs sediment transport to the coast, resulting in sediment deposition and delta progradation^{42,43}.

Thermal abrasion. Thermal abrasion is an effective erosion mechanism along ice-rich permafrost coasts, where the thermal energy of seawater works in combination with wave-driven mechanical energy upon the coast^{25,60,65,67,68}. The water temperature, wave period, and the ground-ice and permafrost properties of the coast determine the effectiveness of thermal abrasion^{67,69}.

The process of thermal erosion along ice-rich coasts is three to four times more effective^{67,69}, compared with coastal abrasion of comparable non-frozen sediments.

As with thermal denudation, thermal abrasion is especially efficient along ice-rich coasts, such as those of the Laptev Sea, where the two processes work interdependently at the bluff top and bluff toe, respectively. During the time period 2010–2013, bluff-top retreat rates along the Laptev coast were found to average 10.2 m per year, whereas bluff-toe retreat rates averaged 3.4 m per year⁶⁶. If the bluff top continues to retreat much faster than the bluff toe, a terrace develops, which contains a mud pool built out of thawed bluff face material. This terrace moves downslope towards the ocean, usually creating a mud lobe, creating a retrogressive thaw slump⁶⁴ (FIG. 1e). Between 1952 and 2011 along the Canadian Beaufort coast, coastal retrogressive thaw slumps increased by 73% in number and by 14% in spatial coverage⁷⁰.

Thermo-erosional niche formation is another process initiated by the thermal abrasion of unlithified, ice-rich bluff toes⁷¹. Niche depth is determined by nearshore oceanographic conditions, including water temperature, storm duration and water level. If the permafrost is penetrated by ice wedges, thermo-erosional niche formation can lead to block failure, which describes the failure of a bluff along the longitudinal axis of an ice wedge, resulting in the toppling of a whole tundra block into the ocean^{72,73} (FIG. 1d). The bluff height, soil strength and ice wedge location mainly define the vulnerability of the bluff to block failure⁷². The failed blocks provide temporary protection to adjacent coastal bluffs, but the failed blocks are usually eroded within days to weeks^{29,57}. Block failure is a critical erosional process along unlithified, ice-rich coasts with bluff heights up to 15 m. Coastal erosion due

to block failure is an episodic process mainly linked to storms⁵⁷, as the precondition for thermo-erosional niche formation is the contact of a bluff toe with water. Block failure is responsible for some of the highest erosion rates in the Arctic, reaching 48.8 m at Drew Point on the US Beaufort coast in the year 2008 (REF.²⁹).

Wave energy. The amount of wave energy transmitted to the shore is determined by the wave period and height, as well as by sea-ice coverage and the duration, frequency and seasonal timing of storms^{74,75}. As with lower-latitude systems, the energy of wind-driven waves is determined by wind speed, wind direction, fetch and the nearshore bathymetry^{14,65}. In the Arctic Ocean, wave fetch greatly depends on sea-ice extent, which has, historically, reached its minimum extent in September and maximum extent in March²² (FIG. 2).

Furthermore, the interplay between sea ice and wave action upon the coast is influenced by the combination of fast ice onset or break-up and the occurrence and timing of storms⁶⁵. In many locations around the Arctic, including the Barents, Kara, Laptev, Chukchi and Beaufort seas, the strongest storms occur in autumn, during September and October^{56,61}. This timing coincides with maximum near-surface ground temperatures and active layer thickness^{76,77}, making the coast susceptible to rapid erosion.

During the open-water season, currents and long-shore wave energy fluxes are important drivers in sediment transport and redistribution⁷⁸. Sea-ice push and rafting are critical mechanisms of sediment transport both along shore and offshore during the spring and fall seasons. In summer, sea ice can be blown to shore by strong winds^{79,80}, leading to wave attenuation⁸¹.

River sediments. Arctic coastal dynamics are further influenced by sediment delivered by Arctic rivers, as this material makes up a large portion of the nearshore coastal sediment budget. Riverine sediment delivery exhibits large daily and seasonal fluctuations⁸². Daily variations in sediment flux can occur due to increasing freshwater run-off from glaciers. Seasonal variations in sediment flux are a consequence of higher run-off during spring break-up and in the warmest months, whereas little to no run-off takes place when rivers are frozen during the winter season⁸³. The largest rivers, including the Ob, Yenisei and Lena rivers in Siberia and the Mackenzie River in Canada, also influence spatial and temporal dynamics in surface salinity, which is an important factor in coastal permafrost erosion, due to its influence on the freeze-thaw point of sediments^{84–86}.

Sea level. Short-term and long-term fluctuations in sea level exert a critical control over shoreline changes and sediment deposition. Eustatic sea-level changes are induced by the change of masses or volume of sea-water, whereas processes affecting relative sea level include glacio-isostatic adjustment, tectonics, thaw subsidence and other processes of water and land mass redistribution^{87–89}. An increase in sea level leads to an increase of wave energy transmission to the coast and, additionally, can increase the effectiveness of thermal

abrasion because waves reach higher portions of the bluff, which were not impacted before. Aside from long-term changes in relative sea level, temporary increases of local sea level, for example, during storms, can evoke immediate shoreline movements and changes in the beach and nearshore profile. A micro-tidal regime characterizes the majority of Arctic coasts⁹⁰, thus, tides have little influence on coastal processes. Extreme storm surges cause increase thermal abrasion of the coast⁹¹ and induce sediment transport⁹² by surge waves, but also lead to flooding and enhanced thawing of the ground in flooded areas^{23,93}.

Each stretch of coast is unique in terms of the composition and the interplay of local coastal characteristics, the regional coastal setting and environmental drivers, which in combination lead to the observed high diversity of Arctic coasts and high variability of shoreline change rates. The presence of ice onshore and offshore increases the complexity of coastal processes along Arctic coasts in comparison with temperate coasts. The factor, or composition of factors, that governs coastal change varies along the coast, which can lead to difficulties in upscaling locally determined shoreline change rates and projecting coastal changes.

Climate sensitivity of Arctic coasts

Permafrost temperatures have warmed over 2007–2016 (REF.⁹⁴). Warming has led to widespread permafrost thaw, ground-ice melt and thermokarst development^{95,96}. Permafrost degradation and thermal denudation are important factors in controlling coastal bluff erosion in the Arctic^{24,25,66} (FIG. 4). Warming permafrost leads to active layer deepening and the delayed onset of freeze-up, reducing the bluffs' resistance to thermal abrasion^{97,98}. Where ground ice is present, permafrost degradation and ground-ice melt can lead to surface subsidence and ground collapse². Permafrost degradation and ground-ice melt have widespread implications for hydrology, moisture exchange, vegetation growth, enhanced coastal erosion and coastal flooding⁹⁹. These implications result in a salt-killed tundra, considerable ecosystem modification and freezing-point depression of the inundated ground^{100–103} (FIG. 5). Where inundated ground contains permafrost and ground ice, subsea permafrost thaw and ground-ice melt occur after flooding, resulting in the lowering and steepening of the nearshore profile¹⁰⁴. Such changes in nearshore bathymetry allow more wave energy to be transmitted to the shore, resulting in higher erosion and more extensive flooding^{53,105,106}. However, the effect of subsea permafrost thaw in the nearshore zone on coastal erosion is considered to be minor^{107,108}.

Sea-surface temperature. Sea-surface temperatures are rising throughout much of the Arctic¹⁰⁹. The effectiveness of increasing solar radiation and air temperature on raising ocean temperature is influenced by oceanic and atmospheric factors, such as sea-ice distribution, ocean optical properties and cloud cover¹¹⁰.

In the Barents and Chukchi seas, the advection of warm water from the North Atlantic and North Pacific oceans, respectively, also contributes to raising ocean temperature¹¹⁰. Furthermore, increasing sea-surface

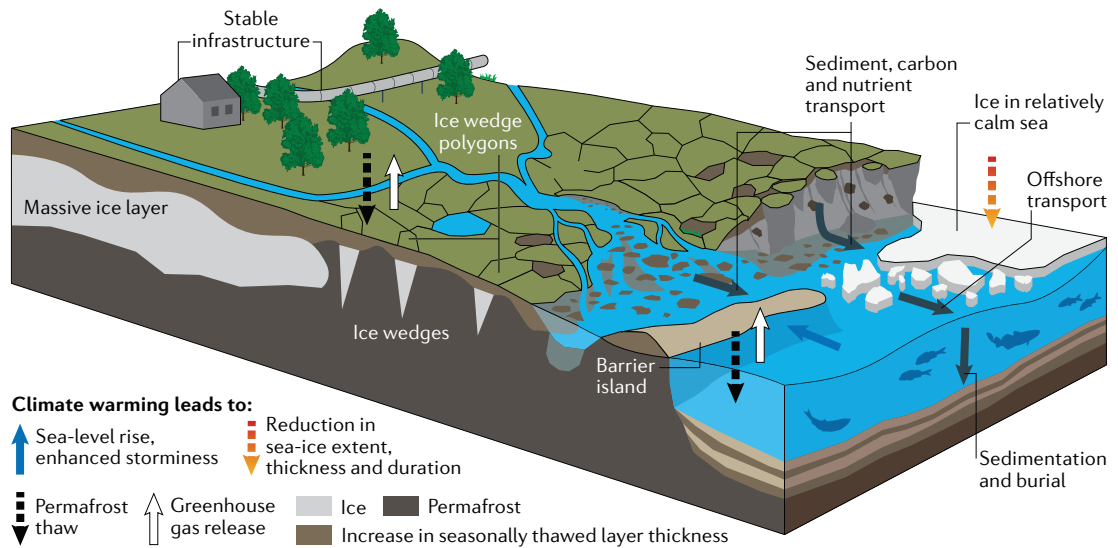


Fig. 4 | Physical processes that contribute to morphodynamic changes along permafrost coasts. Rates of shoreline change are increasing under the influence of a warming climate. Increasing air temperatures and occurrence of flooding from streams and the ocean contribute to permafrost degradation and ground subsidence. Increasing sea levels, higher and more frequent extreme water levels and more powerful waves contribute to accelerating erosion of the Arctic coast. Along ice-rich permafrost coasts with medium bluff heights and narrow beaches, the process of block failure can occur mainly during storms. Adapted from REF.²⁰, Springer Nature Limited.

temperatures contribute to the lengthening of the sea-ice-free period¹¹⁰. In the Chukchi Sea, the mean August sea-surface temperature has risen at a rate of 0.7 °C per decade between 1982 and 2017 (REFS^{10,111}). While the overall trend in Arctic Ocean temperature is positive, multi-decadal variations in ocean temperature have been observed in the Barents Sea, with generally colder temperatures at the beginning of the last century and during the 1970s¹¹². Between the 1970s and the late 2000s, the Barents Sea has experienced an increase in temperature of 4 °C at 100–150 m depth¹⁰. An increase in ocean water temperature enhances the thermo-erosional energy of the water, leading to more effective erosion of ice-rich permafrost bluffs and subsea permafrost degradation¹¹³.

Open-water period. The reduction in sea-ice extent and lengthening of the open-water season lead to longer fetch and to a longer exposure of the coast to wave action. These changes in sea ice directly control the physical vulnerability of the coast to erosion because they lead to the development of long swell waves and higher wind sea states, which additionally increase the frequency and intensity of storms^{1,22,74,114,115}.

Over the satellite-based observational record that started in 1979, Arctic sea ice has generally decreased in extent and in thickness^{19,116,117}. The winter sea-ice maxima during 2015 to 2020 were at record low levels^{19,118} and sea-ice volume in September, when sea-ice cover is at a minimum in the Northern Hemisphere, has declined by 75% since 1979 (REF.¹⁰). Along the Alaskan Beaufort coast, open-water periods have more than doubled in length since the 1980s, from ~45 days in 1979 to ~95 days in 2009 (REF.³). Similarly, along the south-east Chukchi coast, the open-water period has lengthened by 10 days per decade between 1979 and 2016 (REF.¹³).

Along the Laptev and East Siberian coasts, the open-water periods increased from 20 to 30 days between 1979 and 2018 (REF.¹¹⁹). Along the Barents and Kara coasts, open-water periods have become 30 to 40 days longer since the 1970s–1980s. Along the coast of Franz Josef Land, the open-water periods lengthened by 50 days between 1979 and 2015 (REFS^{65,120}).

Wave climate. The reduction of sea-ice extent and lengthening of the open-water season, together with climate-warming-induced changes in the atmosphere, have a great impact on the Arctic Ocean wave climate^{3,59,114,115,121}. Mean near-surface wind speeds over the Arctic Ocean are projected to strengthen locally by up to 50% during the fall and winter seasons, with most extreme wind speeds doubling in frequency¹²¹. Projections of the annual maximum significant wave height amount up to a twofold to threefold increase along some coasts, which will increase the wave-driven erosion and flooding probability. Extreme wave events are projected to particularly increase along the Beaufort coast, where a once-in-20-year event (1979–2005) is projected to occur every 2–5 years in the future (2081–2100)¹¹⁵. As the Beaufort coast is mainly characterized by low, ice-rich bluffs (<10 m in height) and narrow beaches, the projected storm increase has great potential to intensify coastal erosion and sediment redistribution considerably.

The lengthening of the open-water period into the autumnal storm season^{58,122}, combined with rising sea level and increasing fetch, storm frequency⁶¹ and intensity⁶⁰, will lead to increasing length and frequency of high water levels and intensification of erosive wave action. The combined action of coastal exposure, more wave energy and intensifying permafrost degradation will inevitably lead to a further intensification of erosion along the great majority of all permafrost coasts.

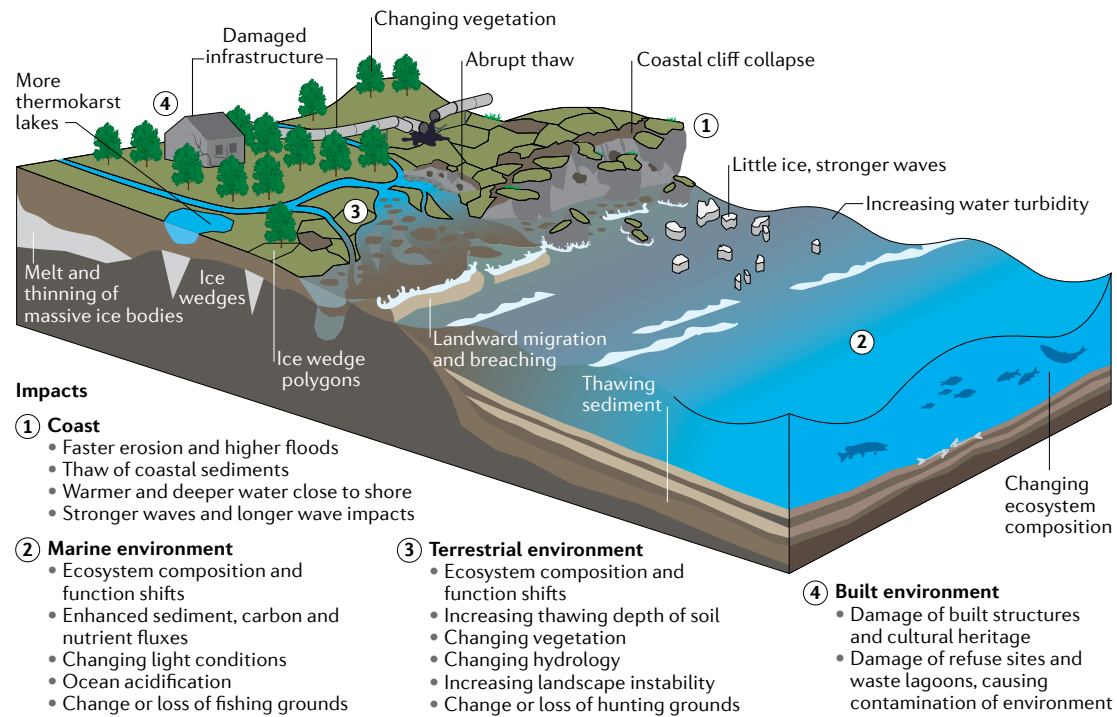


Fig. 5 | Impacts of climate warming on Arctic coastal environments. Schematic of the impacts on the Arctic coast, marine, terrestrial and built environments due to intensified physical processes driven by a warming climate (FIG. 4). (1) Warmer water and air temperatures, as well as higher and more frequent extreme wave and high water-level events, lead to more rapid coastal erosion and destructive coastal flooding. (2) Increasing erosion rates and fluvial sediment delivery increase carbon and nutrient fluxes to the nearshore environment, altering ecosystem composition and services. (3) Higher air and water temperatures contribute to greater thaw depths, permafrost degradation, changes in surface and subsurface flows, and, consequently, changes in vegetation and ecosystem composition and services. (4) Eroding coasts and subsidence of the land surface destabilize built infrastructure, damage or cause the total loss of cultural artefacts and sites, and reroute surficial and subsurface hydrology that can potentially drain or contaminate drinking water supplies. Adapted from REF.²⁰, Springer Nature Limited.

Arctic shoreline changes

The pace and way in which Arctic coasts change depend on the interplay of local coastal characteristics, the regional setting and the intensity of environmental drivers. While some rock coasts are stable over decades, other coasts are characterized by highly dynamic barrier islands or quickly eroding permafrost bluffs. A common method for comparing coastal changes is by measuring the distance between shoreline positions in different years and reporting the annual average distance in metres per year.

Shoreline change. Historical and research biases have led to the majority of shoreline change observations in the Arctic focusing on discrete sections of unlithified erosive coasts, primarily ice-rich permafrost bluffs. Examples include Drew Point, Elson Lagoon and Barter Island on the US Beaufort coast, Herschel Island on the Canadian Beaufort coast, Baydaratskaya Bay on the Kara coast and Muostakh Island on the Laptev coast^{24,26,29,123–126}. Less work has focused on, or included, stable or accretional landforms^{13,27,42,43,55}, lithic coasts^{127,128} or the interaction of landforms along more extensive stretches of coasts^{27,55,91,129,130}. This bias is due, in part, to the general stability of lithic coasts and that the impacts of accumulation processes along coasts are

usually less harmful to both the human and the natural environments.

Data acquisition was very expensive when analyses of Arctic shoreline change began in earnest from the early twentieth century. These constraints led to focus on discrete sections of the coast. These coastal sections often bordered settlements or areas of infrastructure development for military purposes, such as the Distant Early Warning Line stations along the northern border of North America during the Cold War. Sources for historical shoreline positions include geodetic measurements, aerial photographs and topographic maps. Developments in remote sensing technology, such as optical satellite imagery and satellite-derived radar data and unmanned aerial vehicle technologies, have produced increasingly high-spatiotemporal-resolution data, allowing for more comprehensive coastal analyses (FIG. 6). This improvement in technology has provided new insights into changes of shoreline position^{29,124}, geomorphology (FIG. 6), sediment¹³¹ and dissolved organic matter¹³² dispersal dynamics. Remote sensing technologies allow for the investigation of areas that were not investigated previously, such as the Canadian Archipelago¹³³, and remotely access areas independent of weather conditions, for example, cloud coverage¹³⁴.

A wide variety of shoreline proxies are used to identify shoreline movement. The selection of a shoreline proxy depends on the purpose of the shoreline change analysis, as well as available data, data quality and the coastal morphology. Common shoreline proxies for determining shoreline change along coasts are the instantaneous land–water line, the bluff top line, bluff toe line and the vegetation line¹³⁵. Cross-study and cross-proxy comparisons of rates of shoreline change need to account for different uncertainties, which arise from the delineation of the shoreline. Such uncertainties can include using a respective proxy, the duration of observation periods, the extent of shoreline for which shoreline change rates are calculated and the nature of processes, which determine the dynamics of the respective shoreline proxy.

A comparison of shoreline change rates across the Arctic coast shows high spatial and temporal variability, the overwhelming majority of permafrost coasts being erosive (FIG. 2). Shoreline change rates have been increasing since at least the beginning of the 2000s at key observation sites where long-term records exist⁴. Long-term, decadal-scale (ca. 1950s to ca. 2000s) shoreline change rates across the entire Arctic Basin average -0.5 m per year (negative values indicating erosion here and throughout), ranging from 12 to -9 m per year⁵.

Eroding coasts. The highest average decadal-scale rates of coastal erosion occur along the US and Canadian Beaufort coasts, with a mean shoreline change rate of -1.8 m per year (1940s–2010)¹²⁹ along the US coast and -0.7 m per year (1951–2011)²⁷ along the Canadian coast.

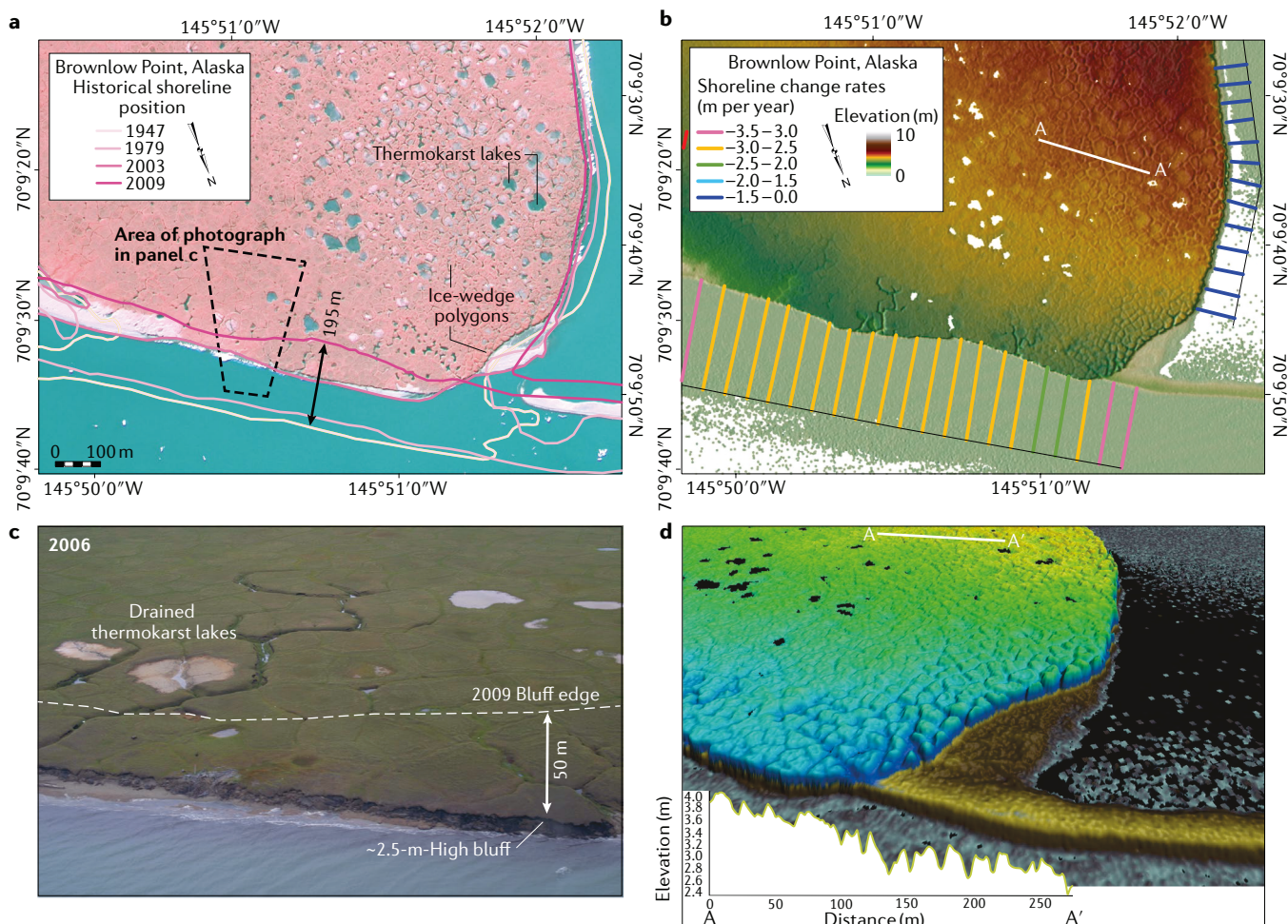


Fig. 6 | Changes to an ice-rich permafrost coast characterized by thermokarst lakes and ice wedges as derived from remote sensing technology. Developments in remote sensing technology, such as space-borne imagery and unmanned aerial vehicle technologies, have produced increasingly high-spatiotemporal-resolution data, allowing for more comprehensive coastal analyses. **a** | Shoreline positions from 1947 to 2009 derived from aerial photography and satellite imagery of a typical coastal permafrost landscape at Brownlow Point on the Beaufort coast of Alaska. Numerous thermokarst lakes and ice-wedge polygons atop a 2.5-m-high tundra bluff are apparent in a colour infrared satellite image from 2003. Historical shoreline changes are shown by coloured lines¹²⁹. Note how the exposed, open-ocean-facing coastal bluff (north is

down in the photo) retreated nearly 200 m over 62 years, between 1947 and 2009. **b** | LiDAR topographic survey of Brownlow Point from 2009. Long-term shoreline change rates (coloured lines perpendicular to the shore) are calculated every 50 m alongshore, reaching up to 3.5 m per year¹²⁹. **c** | An oblique aerial photo taken in 2006 (REF. ¹⁸³), showing drained thermokarst lakes and drainage gullies forming around degrading ice-wedge polygons. Area of photo shown in panel a. **d** | A vertically exaggerated, colour-coded digital elevation model to the south-east of the Brownlow Point headland and adjacent barrier spit. The topographic cross section A–A' shows the complexity of the tundra surface across the ice-wedge polygons. Panel b photo by Bruce Richmond/Ann Gibbs, U.S. Geological Survey.

The US and Canadian Beaufort coasts show the highest percentage increase in shoreline change rates throughout the Arctic, from 80 to 133%^{4,136} and 117 to 160%^{27,124,126}, respectively, when rates of change are compared between 1970s–2000s and 2000s–2010s.

The range of decadal-scale shoreline changes is highest along exposed barrier islands and spans from -22.5 m per year to 20.6 m per year (1980s–2010s) along the US Beaufort coast¹²⁹ to -7.2 m per year to 5.3 m per year (1950s–2011) along the Canadian Beaufort coast²⁷. However, shoreline change rates of gravel features such as barrier islands, bars and spits do not always adequately capture the process of erosion and accretion but, rather, reflect the dynamic sediment transport processes, which lead to gravel feature migration in the direction of longshore drift¹³⁷. Analyses of the size and volume of gravel features would allow for a more comprehensive capture of erosion and accretion processes²⁷.

The Beaufort coast is mainly characterized by actively eroding permafrost bluffs, which recede at a high speed, with up to 48.8 m per year (2007–2008) along the US Beaufort coast²⁹ and up to 8.9 m per year (2014–2015) along the Canadian Beaufort coast²⁷. Along some sheltered stretches of the coast where the combined action of permafrost thaw settlement and sea-level rise act upon the coast, an intensification in erosion is observed through time. Along the US Beaufort coast, rapidly inundating tundra leads to shoreline retreat of up to 25.1 m per year (1980s–2010s)¹²⁹ and of up to 5.8 m per year (1950–2011) along the Canadian Beaufort coast²⁷. The Beaufort coast lies entirely in the continuous permafrost zone and is characterized by unlithified backshore material with high ground-ice contents and relatively low backshore elevations of less than 10 m throughout most parts of the coast. These local characteristics, paired with intensifying environmental drivers such as warming air temperatures and a lengthening of the open-water season (1 to 3.4 days per year between 1979 and 2012)²², render this coast particularly vulnerable to intensifying erosion.

The generally higher rates of coastal erosion along the US Beaufort coast compared with the Canadian Beaufort coast can arise from a generally lower backshore elevation and greater exposure of the coast towards the most frequent and powerful storms. A longer open-water season can also be a factor, because shore-fast ice persists for longer along sheltered stretches of the Canadian Beaufort coast compared with the US Beaufort coast.

The US portion of the Chukchi coast reveals low shoreline change rates, averaging -0.2 m per year (1950–2010s), with no significant difference in the average shoreline change rate in comparison with the 1980s–2010s time period⁵⁵. The highest rates of shoreline change, ranging from -16 m per year to 20 m per year (1980s–2010s), were mostly measured along the highly dynamic barrier island coast, and primarily associated with island migration and formation of inlets⁵⁵. Thirty-seven percent of the Chukchi coast was progradational over the 1980s–2010s time period⁵⁵. Prograding beach ridges along vast stretches of the coast, such as at Point Hope, Cape Krusenstern and Cape Espenberg point to a relatively low wave energy environment paired

with high sediment supply. Only around 10% of the US Chukchi coast is characterized by actively eroding permafrost bluffs, which lead to the overall high rates of shoreline change along the Beaufort coast.

Shoreline change rates along the Russian Arctic coast show a general pattern of increasing mean annual erosion from the mostly non-permafrost-affected, ice-poor, unlithified coast of the western seas (Barents Sea, Kara Sea) to the permafrost-affected, ice-rich, unlithified shoreline of the eastern seas (Laptev Sea, East Siberian Sea, Chukchi Sea)¹¹⁹. Mean shoreline change along the western seas ranges from -0.1 to -4.6 m per year (multiple time periods between 1948 and 2016), whereas mean annual shoreline change along the eastern seas ranges from -0.1 to -11.1 m per year (multiple time periods between 1965 and 2011)¹¹⁹.

Similar to the US Chukchi coast, the permafrost-affected coast along the Russian Chukchi Sea shows small, decadal-scale shoreline changes, which, on average, retreats at ca. -0.4 m per year (1967–2014)¹³⁸. Erosion rates on the Barents coast increased by 50% over 1961–1998 and 1998–2012 (REF.²³), and from 33% to 97% between 1960–2010 and 2010–2016 on the Kara coast^{25,26,139}. Two sites along the Laptev coast showed an increase in erosion rates from 43% to 76% between 1982–2000 and 2000–2018, one of which, Muostakh Island, recorded the highest mean decadal-scale erosion rate in Russia, of -9.5 m per year¹¹⁹. Along the East Siberia coast, shoreline retreat increased by 107% to 129% between 2001 and 2013 (REF.¹⁴⁰).

Stable and prograding coasts. Along the coasts of the Canadian Archipelago, the eastern Canadian Arctic and Hudson Bay, postglacial isostatic uplift exceeds sea-level rise, leading to widespread coastal progradation. Along the north-eastern coast of Hudson Bay, the glacio-static uplift rate amounts to 13 mm per year, whereas global sea-level rise occurs at a speed of approximately 3 mm per year⁴⁹. Analyses of raised gravel beaches in the Canadian High Arctic show progradation rates of 0.1 to 3.9 m per year (1958–2006, 1992–2006), whereas the shoreline also retreats in convex segments of the coast that are exposed to higher wave energy¹³³.

Large parts of Greenland's coast are glaciated, with deglaciated rocky and sedimentary shorelines being intertwined with glaciated stretches of coast throughout the entire island. Even though no extensive analysis of the entire Greenlandic coast has been completed, the deglaciated coast is considered to be stable to prograding, owing to isostatic uplift and delta progradation^{43,49,133}. Progradation of deltas is associated with increasing mass loss from the Greenland ice sheet and was observed to substantially increase in the 1980s to 2010s in comparison with the 1940s to 1980s⁶³.

On Svalbard, the predominantly lithified coast is also considered to be stable¹²⁷. Annual change rates of exposed coastal bluffs measured from 2002 to 2004 span from 2.7 to 3.1 mm (REF.¹⁴¹), and rates of shoreline change measured along beaches span -0.50 to 0.44 m per year between 1936 to 2007 and increased to -0.88 to 0.95 m per year between 2007 to 2017 (REF.¹⁴²), reflecting the generally high natural dynamics of beaches¹³⁵.

A comparison of the different Arctic seas reveals that unlithified permafrost coasts, which are characterized by low bluffs and a high ice content that are directly exposed to wind-driven waves, erode most rapidly with the greatest increase in shoreline change rates since the beginning of the 2000s⁴. Large parts of the Beaufort coast and some stretches of the East Siberian coast meet these conditions (FIG. 3). Highest coastal accumulation rates are found in regions where rapid glacial mass loss results in high sediment supply to the shore and/or in regions that experience isostatic uplift⁴³. Rapidly prograding coasts are primarily situated in Greenland, Svalbard and the Canadian Archipelago^{43,47}.

Arctic coastal evolution reveals high spatial and temporal variability; however, the overwhelming majority of permafrost coasts are erosive. A pan-Arctic correlation between shoreline change rates, multiple environmental drivers and local coastal characteristics continues to be held back by a lack of consistent high-spatiotemporal-resolution shoreline change data and local coastal characteristics data. This lack of a consistent dataset also puts constraints on modelling approaches (BOX 1). The missing pan-Arctic overview of shoreline evolution, in turn, limits the ability to quantify the magnitude of the impact of intensifying climate drivers on Arctic coastal dynamics.

Impacts of Arctic coastal erosion

The impacts of Arctic coastal erosion on the natural environment and the human environment are multi-faceted. Some of the impacts have direct implications,

for example, by destroying coastal settlements, while other impacts are more subtle but also far-reaching, for example, by changing the light availability in the nearshore zone and, thus, potentially impacting primary production.

Impacts on the natural environment. The erosion of permafrost has high potential for environmental impacts owing to the release of organic carbon, nutrients and contaminants to the nearshore zone, offshore and/or the atmosphere when coasts erode^{6–8}. Current estimates put the amount of organic carbon stored in permafrost soils at 1,307 Pg, much larger than the current amount of carbon in the atmosphere (860 Pg)^{143,144}. Current fluxes of organic matter from erosion of permafrost coasts are comparable with that from Arctic river basins¹⁴⁵. The overall annual input of organic carbon from coastal erosion to the Arctic Ocean is estimated to be 14.0 Tg, higher than the amount of particulate organic carbon provided by Arctic rivers⁸².

Furthermore, each year coastal erosion contributes an estimated 1.6 Tg of total nitrogen and 15.4 Tg of carbon to the Arctic Ocean⁷. Unlike large rivers, where decadal to centennial discharge fluctuations can be constrained to a ±10% window^{10,146}, coastal erosion fluxes have the potential to increase by an order of magnitude on the same timescale¹⁴⁶. Such increases would potentially boost primary production, shift nearshore food webs and require local communities that rely on marine biological resources for food security to adapt. The first numbers on ecosystem impacts estimate that one-third of the current Arctic Ocean primary production is sustained by rivers and coastal erosion⁷. There is still a lack of understanding of the potential for coastal erosion to alter coastal ecosystems, for example, due to changes in nutrient availability and water turbidity, which diminishes light intrusion. These are two important preconditions for primary production, an essential component for the whole marine food web on which, for example, local subsistence economies rely^{147,148}.

In addition to regional-scale impacts, increasing coastal erosion can contribute to global-level feedbacks. Organic matter mobilized by the disruption of the soil column during coastal erosion is also emitted as greenhouse gases, resulting in fluxes of CO₂ and CH₄ from coastal bluffs and the water column to the atmosphere^{149–151}. Laboratory incubation experiments indicate that rates of CO₂ emissions from permafrost mixed with seawater exceed terrestrial emission rates of emissions from land^{150,152}. These fluxes have also been observed at eroding coastal bluffs¹⁵³ and indicate that emissions begin immediately when coastal erosion releases organic carbon from permafrost. The magnitude of these coastal-erosion-induced fluxes has not yet been estimated.

Decreasing sea-ice extent and duration will allow the influence from Arctic river discharge to grow, with implications for sediment and nutrient fluxes and, consequently, marine ecosystems^{20,154}. Large uncertainties remain on the fate of organic matter in the water column. Sediment and organic matter in particulate and dissolved forms are reworked by waves in the nearshore

Box 1 | Arctic coastal morphodynamic models fall short on meeting science needs

Whereas Arctic coasts host a diverse mix of geomorphic variability, little work has been done to develop appropriate models that address the morphodynamics of low-lying coastal plain deposits, beaches, beach ridge complexes, deltas, spits and barrier islands with sporadic to continuous permafrost. For example, in only a few instances have Arctic barrier island mobility^{184,185} and erosion of permafrost banks in deltaic environments^{186–188} been examined and modelled. It is only within the past decade that progress been made in developing models to simulate recession of bluffs that account for mechanical (for example, wave contact) and chemical weathering and thermal denudation of permafrost-laden soils^{9,22,73,189–193}.

Testing of (permafrost bluff) model sensitivities to various environmental drivers indicates that the length of the open-water season and time-varying water levels and wave conditions (and, to a lesser degree, air and sea temperatures) are primary drivers, given continuous geomorphic conditions and lithology^{22,194}. The strong dependency on these environmental drivers and historically poor quality of available wave and water-level time series point to the need for better hindcasting and forecasting of these variables. To that end, great advancements in the field of time-varying pan-Arctic sea-ice extents, wave climates and water levels have been and continue to be made, in large part due to advancements in altimeter technology and processing and Earth system models (ESMs) that account for global-scale atmospheric and oceanic teleconnection patterns^{195–197}. However, ESMs do not currently include nutrient and organic carbon loadings from eroding Arctic coasts, which, in turn, generate feedbacks that affect the atmosphere–ocean teleconnection patterns. The exclusion of these processes limits the accuracy of medium-term and long-term projections, and, as such, inclusion of nutrient and carbon inputs from Arctic land loss into ESMs would greatly improve overall understanding. In particular, for settings where such feedback mechanisms cannot be captured explicitly with known physical equations or parameterizations, machine learning and other artificial intelligence techniques might help to bridge the gap between local observations in the Arctic and global state-of-the-art ESMs¹⁹⁸.

zone, resuspended and, eventually, used by organisms, buried on the sea floor, released as greenhouse gases or exported offshore^{20,155,156} (FIG. 4).

The exact role of each of the above-mentioned environmental impacts can vary from one coastal location to another, adding to the level of complexity, and highlighting the need to understand individual coastal environments (for example, river deltas, marshes and the nearshore) within the context of the entire coastal ecosystem. Only when the burial, export and turnover processes for each of these environments can be clearly separated will reliable sediment and organic matter budgets along Arctic coasts be possible. These will help to better predict how coastal-erosion-derived nutrient and organic matter fluxes lead to changes in marine ecosystems through changes of light and nutrient availability, and are an important step towards integrating carbon and nutrient loadings from Arctic land loss into Earth system models (ESMs) (BOX 1).

Impacts on the human environment. The acceleration in coastal erosion induces rapid changes in the coastal environment, creates risks for subsistence-based lifestyles¹⁵⁷ and threatens cultural heritage^{126,158,159}, coastal communities^{157,160} and infrastructure hubs^{161,162}. Risks include the destruction of buildings and roads, loss of access to traditional hunting grounds and destruction of archaeological remains and cultural sites. In the early 2000s, the airstrip at Kaktovik, Alaska was relocated to higher ground, in part, because of repeated coastal flooding¹⁶³. Between the early 1950s and 2011, 26% of all archaeological remains and cultural sites along the Canadian Beaufort coast were destroyed by coastal erosion¹⁵⁸. The fast migration and erosion of the Alaskan North Slope barrier islands affect local subsistence hunting-related ecosystem services, such as wildlife habitats, shelters and locations for camps¹⁵⁷.

Changes in the local or regional climate and environment impact people locally — around 4.3 million people will have to deal with the consequences of previously solid ground thawing beneath their feet. Of these people, 2.2 million live in close proximity to the coast¹⁶⁴ and also need to respond to increasingly dynamic shoreline changes. Along the coast, warming temperatures and thawing and subsiding ground can lead to catastrophic failure of coastal bluffs^{29,91}, damaging buildings and roads^{161,165}, and leading to the destruction of local structures such as traditional ice cellars used for storing food¹⁶⁶. Damage caused by permafrost thaw in coastal settlements will differ depending on the extent of permafrost, permafrost's vulnerability to thawing and future climate trajectories. Coastal settlements are proportionally more exposed to permafrost thaw than inland settlements and, additionally, are at risk from the compounded effects of permafrost degradation, erosion and flooding¹⁶⁴.

The hamlet of Tuktoyaktuk at the Canadian Beaufort coast has attracted international attention because of the damage resulting from coastal erosion. Despite various coastal protection efforts, the seaward part of Tuktoyaktuk has been intensely eroded to the point that houses need to be moved and a graveyard is falling

into the sea. A long-standing discussion on strategic responses has resulted, including the relocation of parts of the hamlet¹⁶⁷.

Several communities have been assessed as critical to relocate in Alaska, including Kivalina and Shishmaref located on barrier islands exposed to the Chukchi Sea. Between 2006 and 2009, approximately 15.5 million US\$ was spent on erosion mitigation efforts in Kivalina¹⁶⁸. Similarly, between 1973 and 2009, 16 million US\$ was invested in Shishmaref¹⁶⁸. Such erosion control measures provide temporary protection, but relocation remains the main solution in the long term. However, relocation is problematic due to high costs, cultural and social objections, and geotechnical issues with proposed alternative sites¹⁶⁹.

The greatest damage in the Russian Arctic has been incurred by communities and polar stations constructed during the Soviet era along eroding coastal segments open to the sea. For example, the Marresalya meteorological station on the Kara coast is among the oldest in the Russian Arctic, and was relocated twice due to bluff erosion¹⁷⁰.

Greenland stands out with respect to coastal communities' resilience because most settlements and infrastructure are built on thaw-stable ground and bedrock substrates. It has been estimated that, by 2050, Greenlandic settlements on permafrost will be the least impacted by permafrost thaw compared with the remaining parts of Arctic coastal settlements¹⁶⁴. Few hazardous events with socio-economic consequences have been observed in Greenland in the past decades^{171,172}. However, the ones that do occur can be severe in their destruction. For example, in 2017, a rock avalanche caused by coastal permafrost degradation in western Greenland caused a tsunami that flooded the nearby village Karrat Fjord, tragically killing four people^{171,172}.

Archaeological remains and cultural sites are experiencing increasing pressure from thawing permafrost and coastal retreat^{158,173}. In Greenland, culturally valuable artefacts located along the coast are threatened and will only be protected until late 2100, under current climate conditions¹⁷⁴. Moreover, in Utqiagvik, Alaska, and along the Yukon coast of Canada, coastal erosion has already destroyed several cultural and historical sites, such as historical cabins, shelters, burial grounds and graveyards^{158,175}.

The economic cost of changing lifestyles, behaviours and activities is unknown. At the same time, some of these future changes could bring or are already bringing opportunities. Opportunities are generally cast in spreading economic activity, especially through exploiting resources in previously avoided regions, increasing cruise ship tourism and opening new trans-Arctic shipping routes^{176,177}, both needing corresponding onshore infrastructure such as harbours and exposing remotely located communities to the cruise sector¹⁷⁸. But these new mining opportunities and infrastructure developments also bear environmental risks, for example, by triggering permafrost degradation, breaking up the sea-ice cover, polluting the marine environment and intensifying coastal erosion.

Resilience of coastal settlements to risks associated with changing coastal hazards depends on the geology and geomorphology of the coast, investments in infrastructure, as well as the type and magnitude of change occurring. Many Arctic settlements are located on relatively stable coasts, where, presently, coastal barriers or bays built natural protections from wave action. However, the future stability of these coasts under increasing sea level and storminess, longer open-water periods and increasing permafrost thaw depths would benefit from a thorough assessment in order to increase the communities' capacity to proactively and sustainably adjust to increasingly dynamic coastal changes.

Summary and future perspectives

The presence of ice along the Arctic coast adds to the complexity of coastal processes and makes them particularly vulnerable towards climate warming. The Arctic coast is predominantly composed of unlithified material, which, in most regions, is permafrost-affected and subject to erosion⁴⁵. The nature and magnitude of coastal change depends on the interplay of local coastal characteristics, the regional coastal setting and environmental drivers^{13,27,55,56}. Local coastal characteristics include coastal geomorphology, cryolithological characteristics and the coastal setting describes the coast's exposure towards waves and solar radiation, whereas environmental drivers include air and water temperature⁵⁷, sea-ice dynamics and properties^{22,58}, wave climatology⁵⁹, storm intensity and timing^{60,61}, and sea-level changes⁶².

The pace of environmental change in the Arctic is increasing, resulting in a rapid evolution of the coastal zone, mainly in the form of accelerating coastal retreat. With the continuous decline of sea-ice extent and persistence, model projections suggest that, by 2070, sea ice will cover Arctic coastal regions for only half of the year⁵⁸. The lengthening of the sea-ice-free season, increasing fetch and rising storminess enhance the wave energy that acts upon Arctic coasts^{22,179,180}. These changes will impact both the natural and the human environments through, for example, the release and redistribution of carbon and nutrients to the marine environment, as well as the loss of land that supports communities and infrastructure. Increased collaboration between coastal communities, stakeholders, policymakers and members of the Arctic science research community, across multiple disciplines, will greatly improve projections of, and adaptation strategies for, the effects of climate change on Arctic coasts.

Current understanding of Arctic coastal dynamics continues to be fragmented because the scarcity of high-spatiotemporal-resolution data, especially for environmental drivers and shoreline change rates, prohibits adequately correlating these processes on the regional to pan-Arctic scale. While such datasets are available for some geographic regions (such as northern Alaska), most of the Arctic coast remains poorly mapped (for example, large parts of the East Siberian coast and Canadian High Arctic coast). Pan-Arctic observations of environmental drivers that are consistent between locations, for example, data on the presence of near-shore sea ice, wave parameters, sea-level fluctuations and

vertical land motion, would help to reduce uncertainties in projections of future coastal change.

In addition, more research on nearshore sediment transport pathways and budgets, as well as sediment-ice entrainment and ice push, will improve the understanding of coastal change processes. Higher spatial resolution data would greatly improve modelling of nearshore sediment dynamics, including nearshore bathymetry, subsea permafrost distribution, subsea and onshore sedimentology, and ground-ice distribution. Advances in technology are leading to satellite data being more widely available at an ever-increasing spatiotemporal resolution. Accessible data combined with automated mapping of shoreline capabilities will lead to continued improvement in the accuracy, frequency and extent of shoreline change measurements, which builds the foundation for understanding the role changing Arctic coasts have in global climate feedback mechanisms.

Medium-term to long-term projections of Earth system processes must incorporate cryospheric processes and associated global system feedbacks if they are to produce more accurate projections under different Intergovernmental Panel on Climate Change Shared Socioeconomic Pathway (IPCC SSP) scenarios. The use of global climate models (and, specifically, ESMs that integrate atmosphere, ocean, land, ice and biosphere interactions) provides invaluable data of environmental drivers that can be fed into finer-scale coastal morphodynamic models and coarse-scale comprehensive system analyses. However, ESMs do not currently include the effects of nutrient and organic carbon loadings from eroding permafrost coasts, let alone the erosion and/or accumulation processes themselves.

Yet, organic matter can be stored in marine sediments or released to the nearshore aquatic environment or the atmosphere as greenhouse gases¹⁵⁶, where they result in further warming. The exclusion of these processes is likely to limit the accuracy of medium-term and long-term global-scale environmental change projections. The inclusion of nutrient and carbon inputs and corresponding greenhouse gas emissions from Arctic land loss into ESMs is a high research priority and would greatly improve system understanding and reduce projection inaccuracies for SSP scenarios.

Finally, global geopolitical interests are focused on emerging Arctic economic opportunities, such as opening shipping routes for goods transport and tourism, forcing local communities to adapt to new socio-environmental developments, in addition to coping with emerging impacts from intensifying coastal changes. Interdisciplinary approaches, in collaboration with local communities, stakeholders and policymakers, build the foundation for economic and environmental sustainable community development along Arctic coasts. Future proactive planning of community infrastructure, together with the development and application of adaptation methods to an increasingly dynamic coastal environment, will help to establish or secure good living conditions in Arctic coastal settlements.

IPCC SSP

Scenarios that describe alternative futures of socio-economic development in the absence of climate policy intervention.

1. Nielsen, D. M., Dobrynin, M., Baehr, J., Razumov, S. & Grigoriev, M. Coastal erosion variability at the southern Laptev Sea linked to winter sea ice and the Arctic Oscillation. *Geophys. Res. Lett.* **47**, e2019GL086876 (2020).
2. Lim, M. et al. Massive ice control on permafrost coast erosion and sensitivity. *Geophys. Res. Lett.* **47**, e2020GL087917 (2020).
3. Overeem, I. et al. Sea ice loss enhances wave action at the Arctic coast. *Geophys. Res. Lett.* **38**, L17503 (2011).
4. Jones, B. M. et al. *Arctic Report Card 2020: coastal permafrost erosion* (NOAA, 2020).
5. Lantuit, H. et al. The Arctic coastal dynamics database: a new classification scheme and statistics on Arctic permafrost coastlines. *Estuaries Coast.* **35**, 383–400 (2011). **The initial description of the only pan-Arctic database of Arctic coastal change to date, this paper describes Arctic coastal dynamics at the turn of the century.**
6. Couture, N. J., Irrgang, A., Pollard, W., Lantuit, H. & Fritz, M. Coastal erosion of permafrost soils along the Yukon Coastal Plain and fluxes of organic carbon to the Canadian Beaufort Sea. *J. Geophys. Res. Biogeosci.* **123**, 406–422 (2018).
7. Terhaar, J., Lauerwald, R., Regnier, P., Gruber, N. & Bopp, L. Around one third of current Arctic Ocean primary production sustained by rivers and coastal erosion. *Nat. Commun.* **12**, 169 (2021). **Highlights the importance of coastal erosion on ocean ecosystems and fisheries.**
8. Schaefer, K. et al. Potential impacts of mercury released from thawing permafrost. *Nat. Commun.* **11**, 4650 (2020).
9. Kupilik, M., Ullgren, M. & Brunswick, D. Bayesian parameter estimation for Arctic coastal erosion under the effects of climate change. *IEEE J. Sel. Top. Appl. Earth Obs. Remote Sens.* **13**, 3595–3604 (2020).
10. Arctic Monitoring and Assessment Programme. Arctic climate change update 2019: an update to key findings of snow, water, ice and permafrost in the Arctic (SWIPA) 2017 (AMAP, 2019).
11. Ballinger, T. J. et al. *Arctic Report Card 2020: surface air temperature* (NOAA, 2020).
12. National Snow and Ice Data Center. *Sea Ice Extent Anomalies* (NSIDC, 2021).
13. Farquharson, L. M. et al. Temporal and spatial variability in coastline response to declining sea-ice in northwest Alaska. *Mar. Geol.* **404**, 71–83 (2018).
14. Ogorodov, S. A. et al. Coastal dynamics of the Pechora and Kara Seas under changing climatic conditions and human disturbances. *Geogr. Environ. Sustain.* **9**, 53–73 (2016).
15. Lantuit, H. et al. The ACD classification of Arctic coasts. *Pangaea* <https://doi.org/10.1594/PANGAEA.919573> (2020).
16. Lantuit, H., Overduin, P. P. & Wetterich, S. Recent progress regarding permafrost coasts. *Permafro. Periglac. Process.* **24**, 120–130 (2013).
17. Overduin, P. P. et al. In *Sedimentary Coastal Zones from High to Low Latitudes: Similarities and Differences* (eds Martini, I. P. & Wanless, H. R.) 103–129 (Geological Society of London, 2014).
18. Forbes, D. L. *State of the Arctic Coast 2010* (Helmholtz-Zentrum Geesthacht, 2011). **Provides a comprehensive integration of physical, ecological and socio-economical aspects related to coastal change, and explores factors that influence the capability of Arctic coastal communities to respond to coastal changes.**
19. Perovich, D. et al. Arctic Report Card 2020: sea ice (NOAA, 2020).
20. Fritz, M., Vonk, J. E. & Lantuit, H. Collapsing Arctic coastlines. *Nat. Clim. Chang.* **7**, 6–7 (2017).
21. Kroon, A. et al. Deltas, freshwater discharge, and waves along the Young Sound, NE Greenland. *Ambio* **46**, 132–145 (2017).
22. Barnhart, K. R., Overeem, I. & Anderson, R. S. The effect of changing sea ice on the physical vulnerability of Arctic coasts. *Cryosphere* **8**, 1777–1799 (2014). **Discusses the effect of sea ice on waves and water levels, and how changes in sea ice affect coastal erosion.**
23. Sinitsyn, A. O., Guegan, E., Shabanova, N., Kokin, O. & Ogorodov, S. Fifty four years of coastal erosion and hydrometeorological parameters in the Varandey region, Barents Sea. *Coast. Eng.* **157**, 103610 (2020).
24. Günther, F., Overduin, P. P., Sandakov, A. V., Grosse, G. & Grigoriev, M. N. Short- and long-term thermo-erosion of ice-rich permafrost coasts in the Laptev Sea region. *Biogeosciences* **10**, 4297–4318 (2013).
25. Baranskaya, A. et al. The role of thermal denudation in erosion of ice-rich permafrost coasts in an enclosed bay (Gulf of Kruzenstern, western Yamal, Russia). *Front. Earth Sci.* **8**, 659 (2021).
26. Novikova, A. et al. Dynamics of permafrost coasts of Baydaratskaya Bay (Kara Sea) based on multi-temporal remote sensing data. *Remote Sens.* **10**, 1481 (2018).
27. Irrgang, A. M. et al. Variability in rates of coastal change along the Yukon coast, 1951 to 2015. *J. Geophys. Res. Earth Surf.* **123**, 779–800 (2018).
28. Lim, M., Whalen, D., Mann, P. J., Fraser, P. & Berry, H. B. Effective monitoring of permafrost coast erosion: Wide-scale storm impacts on outer islands in the Mackenzie Delta area. *Front. Earth Sci.* **8**, 561322 (2020).
29. Jones, B. M. et al. A decade of remotely sensed observations highlight complex processes linked to coastal permafrost bluff erosion in the Arctic. *Environ. Res. Lett.* **13**, 115001 (2018).
30. Strzelecki, M. C. et al. Cryo-conditioned rocky coast systems: A case study from Wilczekodden, Svalbard. *Sci. Total. Environ.* **607–608**, 443–453 (2017).
31. Smith, S. L. et al. The changing thermal state of permafrost. *Nat. Rev. Earth Environ.* <https://doi.org/10.1038/s43017-021-00240-1> (2022).
32. Kanevskiy, M. et al. Ground ice in the upper permafrost of the Beaufort Sea coast of Alaska. *Cold Reg. Sci. Technol.* **85**, 56–70 (2013).
33. Schirrmeyer, L. et al. Fossil organic matter characteristics in permafrost deposits of the northeast Siberian Arctic. *J. Geophys. Res. Biogeosci.* **116**, G00M02 (2011).
34. Murton, J. B. Ground-ice stratigraphy and formation at North Head, Tuktoyaktuk Coastlands, western Arctic Canada: product of glacier–permafrost interactions. *Permafro. Periglac. Process.* **16**, 31–50 (2005).
35. Gaglioti, B. V. et al. Aeolian stratigraphy describes ice-age paleoenvironments in unglaciated Arctic Alaska. *Quat. Sci. Rev.* **182**, 175–190 (2018).
36. Rampton, V. N. *Quaternary Geology of the Yukon Coastal Plain* (Geological Survey of Canada, 1982).
37. Dinter, D. A., Carter, L. D. & Brigham-Grette, J. In *The Arctic Ocean Region* (eds Grantz, A., Johnson, L. & Sweeney, J. F.) (Geological Society of America, 1990).
38. French, H. & Shur, Y. The principles of cryostratigraphy. *Earth Sci. Rev.* **101**, 190–206 (2010).
39. French, H. M. & Harry, D. G. Observations on buried glacier ice and massive segregated ice, western arctic coast, Canada. *Permafro. Periglac. Process.* **1**, 31–43 (1990).
40. Fritz, M. et al. Eastern Beringia and beyond: Late Wisconsinan and Holocene landscape dynamics along the Yukon Coastal Plain, Canada. *Palaeogeogr. Palaeoclimatol. Palaeoecol.* **319–320**, 28–45 (2012).
41. Burn, C. R. in *Landscapes and Landforms of Western Canada Beaufort Sea* (ed. Slaymaker, O.) 335–348 (Springer, 2016).
42. Strzelecki, M. C. et al. New fjords, new coasts, new landscapes: the geomorphology of paraglacial coasts formed after recent glacier retreat in Brepollen (Hornsund, southern Svalbard). *Earth Surf. Process. Landf.* **45**, 1325–1334 (2020).
43. Bendixen, M. et al. Delta progradation in Greenland driven by increasing glacial mass loss. *Nature* **550**, 101–104 (2017). **Illuminates understanding of deltaic coastal change as it relates to sea ice and land-based ice mass loss.**
44. St-Hilaire-Gravel, D., Bell, T. J. & Forbes, D. L. Raised gravel beaches as proxy indicators of past sea-ice and wave conditions, Lowther Island, Canadian Arctic Archipelago. *Arctic* **63**, 213–226 (2010).
45. Kasprzak, M. et al. On the potential for a bottom active layer below coastal permafrost: the impact of seawater on permafrost degradation imaged by electrical resistivity tomography (Hornsund, SW Spitsbergen). *Geomorphology* **293**, 347–359 (2017).
46. Szczucinski, W., Zajaczkowski, M. & Scholten, J. Sediment accumulation rates in subpolar fjords—Impact of post-Little Ice Age glaciers retreat, Billefjorden, Svalbard. *Estuar. Coast. Shelf Sci.* **85**, 345–356 (2009).
47. Strzelecki, M. C. et al. The role of rapid glacier retreat and landscape transformation in controlling the post-Little Ice Age evolution of paraglacial coasts in central Spitsbergen (Billefjorden, Svalbard). *Land Degrad. Dev.* **29**, 1962–1978 (2018).
48. Kroon, A. in *Coastal Environments and Global Change* (eds Masselink, G. & Gehrels, R.) 338–355 (Wiley, 2014).
49. Boisson, A., Allard, M. & Sarrazin, D. Permafrost aggradation along the emerging eastern coast of Hudson Bay, Nunavik (northern Québec, Canada). *Permafro. Periglac. Process.* **31**, 128–140 (2020).
50. Hansell, R. I. C., Scott, P. A., Stanforth, R. & Svoboda, J. Permafrost development in the intertidal zone at Churchill, Manitoba: A possible mechanism for accelerated beach uplift. *Arctic* **36**, 198–203 (1983).
51. Angelopoulos, M. et al. Thermokarst lake to lagoon transitions in eastern Siberia: Do submerged taliks refreeze? *J. Geophys. Res. Earth Surf.* **125**, e2019JF005424 (2020).
52. Overduin, P. P. et al. Coastal dynamics and submarine permafrost in shallow water of the central Laptev Sea, East Siberia. *Cryosphere* **10**, 1449–1462 (2016).
53. Iwahana, G., Cooper, Z. S., Carpenter, S. D., Deming, J. W. & Eicken, H. Intra-ice and intra-sediment cryopelagic brine occurrence in permafrost near Utqiagvik (Barrow). *Permafro. Periglac. Process.* **32**, 427–446 (2021).
54. Romanovskii, N. N., Gravis, G. F., Melnikov, E. S. & Leibman, M. O. in *Geoindicators: Assessing Rapid Environmental Changes in Earth Systems* 47–68 (A. A. Balkema, 1996).
55. Gibbs, A. E., Snyder, A. G. & Richmond, B. M. National assessment of shoreline change — historical shoreline change along the north coast of Alaska, Icy Cape to Cape Prince of Wales (US Geological Survey, 2019).
56. Manson, G. K., Solomon, S. M., Forbes, D. L., Atkinson, D. E. & Craymer, M. Spatial variability of factors influencing coastal change in the western Canadian Arctic. *Geomarine Lett.* **25**, 138–145 (2005).
57. Barnhart, K. R. et al. Modeling erosion of ice-rich permafrost bluffs along the Alaskan Beaufort Sea coast. *J. Geophys. Res. Earth Surf.* **119**, 1155–1179 (2014).
58. Barnhart, K. R., Miller, C. R., Overeem, I. & Kay, J. E. Mapping the future expansion of Arctic open water. *Nat. Clim. Chang.* **6**, 280–285 (2015).
59. Casas-Prat, M. & Wang, X. L. Sea ice retreat contributes to projected increases in extreme Arctic ocean surface waves. *Geophys. Res. Lett.* **47**, e2020GL088100 (2020).
60. Manson, G. K. & Solomon, S. M. Past and future forcing of Beaufort Sea coastal change. *Atmos. Ocean* **45**, 107–122 (2007).
61. Atkinson, D. Observed storminess patterns and trends in the circum-Arctic coastal regime. *Geo-Mar. Lett.* **25**, 98–109 (2005).
62. Meyssignac, B. & Cazenave, A. Sea level: A review of present-day and recent-past changes and variability. *J. Geodyn.* **58**, 96–109 (2012).
63. Belova, N. G. et al. Erosion of permafrost coasts of Kara Sea near Kharasavay Cape, Western Yamal. *Earth's Cryosph.* **21**, 85–96 (2017).
64. French, H. M. *The Periglacial Environment* (Wiley, 2017).
65. Shabanova, N. N., Ogorodov, S., Shabanov, P. & Baranskaya, A. Hydrometeorological forcing of western Russian Arctic coastal dynamics: XX-century history and current state. *Geogr. Environ. Sustain.* **11**, 113–129 (2018).
66. Günther, F. et al. Observing Muostakh disappear: permafrost thaw subsidence and erosion of a ground-ice-rich island in response to arctic summer warming and sea ice reduction. *Cryosphere* **9**, 151–178 (2015).
67. Aré, F. E. Thermal abrasion of sea coasts (part I). *Polar Geogr. Geol.* **12**, 1–86 (1988).
68. Frederick, J. M., Thomas, M. A., Bell, D. L., Jones, C. A. & Roberts, J. D. *The Arctic coastal erosion problem* (Sandia National Laboratories, 2016).
69. Aré, F. E. Thermal abrasion of sea coasts (Part II). *Polar Geogr. Geol.* **12**, 87–157 (1988). **A landmark study published in two parts comprehensively describing the effect of ice on coastal dynamics.**
70. Ramage, J. L., Irrgang, A. M., Morgenstern, A. & Lantuit, H. Increasing coastal slump activity impacts the release of sediment and organic carbon into the Arctic Ocean. *Biogeosciences* **15**, 1483–1495 (2018).
71. Kobayashi, N. Formation of thermoerosional niches into frozen bluffs due to storm surges on the Beaufort Sea coast. *J. Geophys. Res. Oceans* **90**, 11983–11988 (1985). **One of the first, or perhaps the first, studies that presents a model of permafrost bluff niching, erosion and recession.**

72. Hoque, M. A. & Pollard, W. H. Arctic coastal retreat through block failure. *Can. Geotech. J.* **46**, 1103–1115 (2009).
73. Hoque, M. A. & Pollard, W. H. Stability of permafrost dominated coastal cliffs in the Arctic. *Polar Sci.* **10**, 79–88 (2016).
74. Thomson, J. et al. Emerging trends in the sea state of the Beaufort and Chukchi seas. *Ocean Model.* **105**, 1–12 (2016).
75. Ahmad, N., Bihs, H., Chella, M. A., Kamath, A. & Arntsen, O. A. CFD modeling of arctic coastal erosion due to breaking waves. *Int. J. Offshore Polar Eng.* **29**, 33–41 (2019).
76. Brown, J., Hinkel, K. M. & Nelson, F. E. The circumpolar active layer monitoring (CALM) program: research designs and initial results. *Polar Geogr.* **24**, 166–258 (2000).
77. Nicolsky, D. J., Romanovsky, V. E., Panda, S. K., Marchenko, S. S. & Muskett, R. R. Applicability of the ecosystem type approach to model permafrost dynamics across the Alaska North Slope. *J. Geophys. Res. Earth Surf.* **122**, 50–75 (2017).
78. Hume, J. D. & Schalk, M. Shoreline processes near Barrow, Alaska: a comparison of the normal and the catastrophic. *Arctic* **20**, 86–103 (1967).
79. Kempema, E. W., Reimnitz, E. & Barnes, P. Sea ice sediment entrainment and rafting in the Arctic. *J. Sediment. Res.* **59**, 308–317 (1989).
80. Hume, J. D. & Schalk, M. The effects of ice push on Arctic beaches. *Am. J. Sci.* **262**, 267–273 (1964).
81. Manson, G. K., Davidson-Arnott, R. G. D. & Ollerhead, J. Attenuation of wave energy by nearshore sea ice: Prince Edward Island, Canada. *J. Coast. Res.* **32**, 253–263 (2016).
82. Wegner, C. et al. Variability in transport of terrigenous material on the shelves and the deep Arctic Ocean during the Holocene. *Polar Res.* **34**, 24964 (2015).
83. Bendixen, M. & Kroon, A. Conceptualizing delta forms and processes in Arctic coastal environments. *Earth Surf. Process. Landf.* **42**, 1227–1237 (2017).
84. Golubeva, E., Platov, G., Iakshina, D. & Kraineva, M. A simulated distribution of Siberian river runoff in the Arctic Ocean. *IOP Conf. Ser. Earth Environ. Sci.* **386**, 012022 (2019).
85. Bauch, D. et al. Correlation of river water and local sea-ice melting on the Laptev Sea shelf (Siberian Arctic). *J. Geophys. Res. Oceans* **118**, 550–561 (2013).
86. Kuzin, V. I., Platov, G. A. & Golubeva, E. N. Influence that interannual variations in Siberian river discharge have on redistribution of freshwater fluxes in Arctic Ocean and North Atlantic. *Izv. Atmos. Ocean. Phys.* **46**, 770–783 (2010).
87. Farquharson, L. et al. Alaskan marine transgressions record out-of-phase Arctic Ocean glaciation during the last interglacial. *Geology* **46**, 783–786 (2018).
88. Horton, B. P. et al. Mapping sea-level change in time, space, and probability. *Annu. Rev. Environ. Resour.* **43**, 481–521 (2018).
89. Lambeck, K., Rouby, H., Purcell, A., Sun, Y. & Sambridge, M. Sea level and global ice volumes from the Last Glacial Maximum to the Holocene. *Proc. Natl Acad. Sci. USA* **111**, 15296–15303 (2014).
90. European Space Agency. *Modelling tides in the Arctic Ocean* (ESA, 2021).
91. Gibbs, A. E., Nolan, M., Richmond, B. M., Snyder, A. G. & Erikson, L. H. Assessing patterns of annual change to permafrost bluffs along the North Slope coast of Alaska using high-resolution imagery and elevation models. *Geomorphology* **336**, 152–164 (2019).
92. Héquette, A., Desrosiers, M., Hill, P. & Forbes, D. The influence of coastal morphology on shoreface sediment transport under storm-combined flows, Canadian Beaufort Sea. *J. Coast. Res.* **17**, 507–516 (2001).
93. Kim, J., Murphy, E., Nistor, I., Ferguson, S. & Provan, M. Numerical analysis of storm surges on Canada's western Arctic coastline. *J. Mar. Sci. Eng.* **9**, 326 (2021).
94. Biskaborn, B. K. et al. Permafrost is warming at a global scale. *Nat. Commun.* **10**, 264 (2019).
95. Farquharson, L. M. et al. Climate change drives widespread and rapid thermokarst development in very cold permafrost in the Canadian High Arctic. *Geophys. Res. Lett.* **46**, 6681–6689 (2019).
96. Liljedahl, A. K. et al. Pan-Arctic ice-wedge degradation in warming permafrost and its influence on tundra hydrology. *Nat. Geosci.* **9**, 312–318 (2016).
97. Lund, M., Hansen, B. U., Pedersen, S. H., Stiegler, C. & Tamstorf, M. P. Characteristics of summer-time energy exchange in a high Arctic tundra heath 2000–2010. *Tellus B Chem. Phys. Meteorol.* **66**, 21631 (2014).
98. Blunden, J. & Arndt, D. S. *State of the Climate in 2016* Vol. 98 (American Meteorological Society, 2017).
99. Heijmans, M. M. P. D. et al. Tundra vegetation change trajectories across permafrost environments and consequences for permafrost thaw. *Nat. Rev. Earth Environ.* <https://doi.org/10.1038/s43017-021-00233-0> (2022).
100. Arp, C. D., Jones, B. M., Schmutz, J. A., Urban, F. E. & Jorgenson, M. T. Two mechanisms of aquatic and terrestrial habitat change along an Alaskan Arctic coastline. *Polar Biol.* **33**, 1629–1640 (2010).
101. Jorgenson, J. C., Raynolds, M. K., Reynolds, J. H. & Benson, A.-M. Twenty-five year record of changes in plant cover on tundra of northeastern Alaska. *Arctic Antarct. Alp. Res.* **47**, 785–806 (2015).
102. Johansson, M., Christensen, T. R., Akerman, J. H. & Callaghan, T. V. What determines the current presence or absence of permafrost in the Torneträsk region, a sub-arctic landscape in northern Sweden? *Ambio* **35**, 190–197 (2006).
103. Torre Jorgenson, M. et al. Reorganization of vegetation, hydrology and soil carbon after permafrost degradation across heterogeneous boreal landscapes. *Environ. Res. Lett.* **8**, 035017 (2013).
104. Dallimore, S. R., Wolfe, S. & Solomon, S. M. Influence of ground ice and permafrost on coastal evolution, Richards Island, Beaufort Sea coast, N.W.T. *Can. J. Earth Sci.* **33**, 664–675 (1996).
105. Aré, F. E. & Reimnitz, E. The A and m coefficients in the Bruun/Dean equilibrium profile equation seen from the Arctic. *J. Coast. Res.* **24**, 243–249 (2008).
106. Angelopoulos, M., Overduin, P. P., Miesner, F., Grigoriev, M. N. & Vasilev, A. V. Recent advances in the study of Arctic submarine permafrost. *Permafrost. Periglac. Process.* **31**, 442–453 (2020).
107. Aré, F., Reimnitz, E., Grigoriev, M., Hubberten, H.-W. & Rachold, V. The influence of cryogenic processes on the erosional Arctic shoreface. *J. Coast. Res.* **241**, 110–121 (2008). **Establishes that profile models used in ice-free environments are conditionally viable for permafrost coasts.**
108. Reimnitz, E., Graves, S. M. & Barnes, P. W. *Beaufort Sea Coastal Erosion, Sediment Flux, Shoreline Evolution, and the Erosional Shelf Profile* (US Geological Survey, 1988).
109. Carvalho, K. S. & Wang, S. Sea surface temperature variability in the Arctic Ocean and its marginal seas in a changing climate: Patterns and mechanisms. *Glob. Planet. Change* **193**, 103265 (2020).
110. Timmermans, M.-L. & Labé, Z. Arctic Report Card 2020: sea surface temperature (NOAA, 2020).
111. Richter-Menge, J. & Druckmiller, M. L. State of the climate in 2019. *Bull. Amer. Meteor. Soc.* **101**, S185–S238 (2020).
112. Levitus, S., Matishov, G., Seidov, D. & Smolyar, I. Barents Sea multidecadal variability. *Geophys. Res. Lett.* **36**, L19604 (2009).
113. Dmitrenko, I. A. et al. Recent changes in shelf hydrography in the Siberian Arctic: Potential for subsea permafrost instability. *J. Geophys. Res. Ocean* **116**, C10027 (2011).
114. Vermaire, J. C. et al. Arctic climate warming and sea ice declines lead to increased storm surge activity. *Geophys. Res. Lett.* **40**, 1386–1390 (2013).
115. Casas-Prat, M. & Wang, X. L. Projections of extreme ocean waves in the Arctic and potential implications for coastal inundation and erosion. *J. Geophys. Res. Ocean* **125**, e2019JC015745 (2020). **Presents the first end-of-twenty-first century, multimodel ensemble of projected extreme waves along the circum-Arctic coast.**
116. Kwok, R. et al. Thinning and volume loss of the Arctic Ocean sea ice cover: 2003–2008. *J. Geophys. Res.* **114**, C07005 (2009).
117. Maslanki, J. A. et al. A younger, thinner Arctic ice cover: Increased potential for rapid, extensive sea-ice loss. *Geophys. Res. Lett.* **34**, 2004–2008 (2007).
118. Comiso, J. C., Meier, W. N. & Gersten, R. Variability and trends in the Arctic Sea ice cover: Results from different techniques. *J. Geophys. Res. Ocean* **122**, 6883–6900 (2017).
119. Ogorodov, S., Aleksyutina, D., Baranskaya, A., Shabanova, N. & Shilova, O. Coastal erosion of the Russian Arctic: An overview. *J. Coast. Res.* **95**, 599–604 (2020).
120. Shabanov, P. A. & Shabanova, N. N. Ice-free period detection method in the Arctic coastal zone. *Russ. J. Earth Sci.* **20**, ES6016 (2020).
121. Mioduszewski, J., Vavrus, S. & Wang, M. Diminishing Arctic sea ice promotes stronger surface winds. *J. Clim.* **31**, 8101–8119 (2018).
122. Box, J. E. et al. Key indicators of Arctic climate change: 1971–2017. *Environ. Res. Lett.* **14**, 45010 (2019).
123. Obu, J. et al. Coastal erosion and mass wasting along the Canadian Beaufort Sea based on annual airborne LiDAR elevation data. *Geomorphology* **293**, 331–346 (2017).
124. Cunliffe, A. et al. Rapid retreat of permafrost coastline observed with aerial drone photogrammetry. *Cryosphere* **13**, 1513–1528 (2019).
125. Lantuit, H. & Pollard, W. H. Fifty years of coastal erosion and retrogressive thaw slump activity on Herschel Island, southern Beaufort Sea, Yukon Territory, Canada. *Geomorphology* **95**, 84–102 (2008).
126. Radosavljevic, B. et al. Erosion and flooding — threats to coastal infrastructure in the Arctic: a case study from Herschel Island, Yukon Territory, Canada. *Estuaries Coast.* **39**, 900–915 (2015).
127. Lim, M. et al. Arctic rock coast responses under a changing climate. *Remote Sens. Environ.* **236**, 111500 (2020).
128. Zagorski, P. et al. Multidecadal (1960–2011) shoreline changes in Isbjörnhamna (Hornsund, Svalbard). *Pol. Polar Res.* **36**, 369–390 (2015).
129. Gibbs, A. E. & Richmond, B. M. *National assessment of shoreline change — summary statistics for updated vector shorelines and associated shoreline change data for the north coast of Alaska, US-Canadian Border to Icy Cape* (US Geological Survey, 2017).
130. Gibbs, A. E. & Richmond, B. M. *National assessment of shoreline change: historical shoreline change along the north coast of Alaska, US-Canadian border to Icy Cape* (US Geological Survey, 2015).
131. Klein, K. P. et al. Long-term high-resolution sediment and sea surface temperature spatial patterns in Arctic nearshore waters retrieved using 30-year Landsat archive imagery. *Remote Sens.* **11**, 2791 (2019).
132. Juhls, B. et al. Dissolved organic matter at the fluvial-marine transition in the Laptev Sea using in situ data and ocean colour remote sensing. *Biogeosciences* **16**, 2693–2713 (2019).
133. St-Hilaire-Gravel, D., Forbes, D. L. & Bell, T. Multitemporal analysis of a gravel-dominated coastline in the central Canadian Arctic Archipelago. *J. Coast. Res.* **28**, 421–441 (2012).
134. Bartsch, A., Ley, S., Nitze, I., Pointner, G. & Vieira, G. Feasibility study for the application of Synthetic Aperture Radar for coastal erosion rate quantification across the Arctic. *Front. Environ. Sci.* **8**, 143 (2020).
135. Boak, E. H. & Turner, I. L. Shoreline definition and detection: a review. *J. Coast. Res.* **214**, 688–703 (2005).
136. Brown, J., Jorgenson, M., Smith, O. & Lee, W. in *Permafrost: proceedings of the 8th International Conference on Permafrost* (A.A. Balkema, 2003).
137. Davidson-Arnott, R. G. D. in *Introduction to Coastal Processes and Geomorphology* (ed. Davidson-Arnott, R. G. D.) 280–324 (Cambridge Univ. Press, 2010).
138. Maslakov, A. & Kraev, G. Erodibility of permafrost exposures in the coasts of Eastern Chukotka. *Polar Sci.* **10**, 374–381 (2016).
139. Belova, N. G., Novikova, A. V., Günther, F. & Shabanova, N. N. Spatiotemporal variability of coastal retreat rates at western Yamal Peninsula, Russia, based on remotely sensed data. *J. Coast. Res.* **95**, 367–371 (2020).
140. Gavrilov, A. V. & Pizhankova, E. I. Dynamics of permafrost in the coastal zone of Eastern-Asian sector of the Arctic. *Geogr. Environ. Sustain.* **11**, 20–37 (2018).
141. Wangensteen, B., Eiken, T., Odegård, R. S. & Sollid, J. L. Measuring coastal cliff retreat in the Kongsfjorden area, Svalbard, using terrestrial photogrammetry. *Polar Res.* **26**, 14–21 (2007).
142. Zagorski, P., Jarosz, K. & Superson, J. Integrated assessment of shoreline change along the Calypsostranda (Svalbard) from remote sensing, field survey and GIS. *Mar. Geod.* **43**, 433–471 (2020).
143. Hugelius, G. et al. Estimated stocks of circumpolar permafrost carbon with quantified uncertainty ranges and identified data gaps. *Biogeosciences* **11**, 6573–6593 (2014).
144. Friedlingstein, P. et al. Global carbon budget 2020. *Earth Syst. Sci. Data* **12**, 3269–3340 (2020).
145. Rachold, V. et al. Coastal erosion vs riverine sediment discharge in the Arctic Shelf seas. *Int. J. Earth Sci.* **89**, 450–460 (2000).
146. Wagner, A., Lohmann, G. & Prange, M. Arctic river discharge trends since 7 ka BP. *Glob. Planet. Change* **79**, 48–60 (2011).

147. Dunton, K. H., Weingartner, T. & Carmack, E. C. The nearshore western Beaufort Sea ecosystem: Circulation and importance of terrestrial carbon in arctic coastal food webs. *Prog. Oceanogr.* **71**, 362–378 (2006).
148. Dunton, K. H., Schonberg, S. V. & Cooper, L. W. Food web structure of the Alaskan nearshore shelf and estuarine lagoons of the Beaufort Sea. *Estuaries Coast.* **35**, 416–435 (2012).
149. Abbott, B. W. & Jones, J. B. Permafrost collapse alters soil carbon stocks, respiration, CH_4 , and N_2O in upland tundra. *Glob. Chang. Biol.* **21**, 4570–4587 (2015).
150. Tanski, G. et al. Permafrost carbon and CO_2 pathways differ at contrasting coastal erosion sites in the Canadian Arctic. *Front. Arctic.* **9**, 630493 (2021).
151. Miner, K. R. et al. Permafrost carbon emissions in a changing Arctic. *Nat. Rev. Earth Environ.* <https://doi.org/10.1038/s43017-021-00230-3> (2022).
152. Tanski, G. et al. Rapid CO_2 release from eroding permafrost in seawater. *Geophys. Res. Lett.* **46**, 11244–11252 (2019).
153. Vonk, J. E. et al. Activation of old carbon by erosion of coastal and subsea permafrost in Arctic Siberia. *Nature* **489**, 137–140 (2012).
154. Janout, M. A. et al. On the variability of stratification in the freshwater-influenced Laptev Sea Region. *Front. Mar. Sci.* **7**, 543489 (2020).
155. Grotheer, H. et al. Burial and origin of permafrost-derived carbon in the nearshore zone of the southern Canadian Beaufort Sea. *Geophys. Res. Lett.* **47**, e2019GL085897 (2020).
156. Jong, D. et al. Nearshore zone dynamics determine pathway of organic carbon from eroding permafrost coasts. *Geophys. Res. Lett.* **47**, e2020GL088561 (2020).
157. Brady, M. B. & Leichenko, R. The impacts of coastal erosion on Alaska's North Slope communities: A co-production assessment of land use damages and risks. *Polar Geogr.* **43**, 259–279 (2020).
158. Irgang, A. M., Lantuit, H., Gordon, R. R., Piskor, A. & Manson, G. K. Impacts of past and future coastal changes on the Yukon coast — threats for cultural sites, infrastructure, and travel routes. *Arct. Sci.* **5**, 107–126 (2019).
159. Jensen, A. M. in *Public Archaeology and Climate Change* (eds Dawson, T., Nimura, C., López-Romero, E. & Daire, M.-Y.) 126–137 (Oxbow Books, 2019).
160. Jaskolski, M. W., Pawłowski, Ł. & Strzelecki, M. C. High Arctic coasts at risk — the case study of coastal zone development and degradation associated with climate changes and multidirectional human impacts in Longyearbyen (Adventfjorden, Svalbard). *Land Degrad. Dev.* **29**, 2514–2524 (2018).
161. Hjort, J. et al. Degrading permafrost puts Arctic infrastructure at risk by mid-century. *Nat. Commun.* **9**, 5147 (2018).
162. Hjort, J. et al. Impacts of permafrost degradation on infrastructure. *Nat. Rev. Earth Environ.* <https://doi.org/10.1038/s43017-021-00247-8> (2022).
163. US Department of the Interior. Biological opinion for the relocation of the Kaktovik Airport (DOI, 2011).
164. Ramage, J. et al. Population living on permafrost in the Arctic. *Popul. Environ.* **43**, 22–38 (2021).
165. Larson, M., Hanson, H., Member, A., Kraus, N. C. & Newe, J. Short- and long-term responses of beach fills determined by EOF analysis. *J. Waterw. Port Coast. Ocean Eng.* **125**, 285–293 (1999).
166. Nyland, K. E. et al. Traditional Inupiat ice cellars (SIQIUAQ) in Barrow, Alaska: characteristics, temperature monitoring, and distribution. *Geogr. Rev.* **107**, 143–158 (2017).
167. Government of Northwest Territories. Alfred Moses: Tuktoyaktuk shoreline relocation project (GNWT, 2018).
168. Bronen, R. & Chapin, F. S. Adaptive governance and institutional strategies for climate-induced community relocations in Alaska. *Proc. Natl. Acad. Sci. USA* **110**, 9320–9325 (2013).
169. Landauer, M. & Juhola, S. *Loss and Damage from Climate Change* (Springer, 2019).
170. Kritsuk, L. N., Dubrovinn, V. A. & Yastreba, N. V. Results of complex study of the Kara Sea shore dynamics in the area of the meteorological station Marre-Sale, using GIS-technologies. *Earths Cryosph.* **18**, 59–69 (2014).
171. Strzelecki, M. C. & Jaskolski, M. W. Arctic tsunamis threaten coastal landscapes and communities—survey of Karrat Isfjord 2017 tsunami effects in Nuugaatsiaq, western Greenland. *Nat. Hazards Earth Syst. Sci.* **20**, 2521–2534 (2020).
172. Svennevig, K. et al. Evolution of events before and after the 17 June 2017 rock avalanche at Karrat Fjord, West Greenland - A multidisciplinary approach to detecting and locating unstable rock slopes in a remote Arctic area. *Earth Surf. Dyn.* **8**, 1021–1038 (2020).
173. O'Rourke, M. J. E. Archaeological site vulnerability modelling: the influence of high impact storm events on models of shoreline erosion in the western Canadian Arctic. *Open Archaeol.* **3**, 1–16 (2017).
174. Elberling, B. et al. Paleo-Eskimo kitchen midden preservation in permafrost under future climate conditions at Qajaa, West Greenland. *J. Archaeol. Sci.* **38**, 1331–1339 (2011).
175. Jones, B. M., Hinkel, K. M., Arp, C. D. & Eisner, W. R. Modern erosion rates and loss of coastal features and sites, Beaufort Sea coastline, Alaska. *Arctic* **61**, 361–372 (2008).
176. Mudryk, L. R. et al. Impact of 1, 2 and 4 °C of global warming on ship navigation in the Canadian Arctic. *Nat. Clim. Chang.* **11**, 29–31 (2021).
177. Smith, L. C. & Stephenson, S. R. New Trans-Arctic shipping routes navigable by midcentury. *Proc. Natl. Acad. Sci. USA* **110**, E1191–E1195 (2013).
178. Stewart, E., Dawson, J. & Johnston, M. Risks and opportunities associated with change in the cruise tourism sector: Community perspectives from Arctic Canada. *Polar J.* **5**, 403–427 (2015).
179. Wöbüs, C. et al. Thermal erosion of a permafrost coastline: improving process-based models using time-lapse photography. *Arctic Antarct. Alp. Res.* **43**, 474–484 (2011).
180. Li, J., Ma, Y., Liu, Q., Zhang, W. & Guan, C. Growth of wave height with retreating ice cover in the Arctic. *Cold Reg. Sci. Technol.* **164**, 102790 (2019).
181. Obu, J., Westermann, S., Kääb, A. & Bartsch, A. Ground temperature map, 2000–2016, Northern Hemisphere permafrost. *Pangaea* <https://doi.org/10.1594/PANGAEA.888600> (2018).
182. Overduin, P. P. et al. Submarine Permafrost Map (SuPerMAP), modeled with CryoGrid 2, Circum-Arctic. *Pangaea* <https://doi.org/10.1594/PANGAEA.910540> (2020).
183. Gibbs, A. E. & Richmond, B. Oblique aerial photography of the Arctic coast of Alaska, Nulavik to Demarcation Point, August 7–10, 2006 (US Geological Survey, 2009).
184. Stutz, M. L. & Pilkey, O. H. Open-ocean barrier islands: global influence of climatic, oceanographic, and depositional settings. *J. Coast. Res.* **27**, 207–222 (2011).
185. Roelvink, D., Huisman, B., Elghandour, A., Ghonim, M. & Reynolds, J. Efficient modeling of complex sandy coastal evolution at monthly to century time scales. *Front. Mar. Sci.* **7**, 535 (2020).
186. Lauzon, R., Piliouras, A. & Rowland, J. C. Ice and permafrost effects on delta morphology and channel dynamics. *Geophys. Res. Lett.* **46**, 6574–6582 (2019).
187. Piliouras, A., Lauzon, R. & Rowland, J. C. Unraveling the combined effects of ice and permafrost on Arctic delta morphodynamics. *J. Geophys. Res. Earth Surf.* **126**, e2020JF005706 (2021).
188. Lim, Y., Levy, J., Goudge, T. & Kim, W. Ice cover as a control on the morphodynamics and stratigraphy of Arctic deltas. *Geology* **47**, 399–402 (2019).
189. Ravens, T. M., Jones, B. M., Zhang, J., Arp, C. D. & Schmutz, J. A. Process-based coastal erosion modeling for Drew Point, North Slope, Alaska. *J. Waterw. Port Coast. Ocean Eng.* **138**, 122–130 (2012).
190. Kupilik, M., Witmer, F. D. W., MacLeod, E., Wang, C. & Ravens, T. Gaussian process regression for Arctic coastal erosion forecasting. *IEEE Trans. Geosci. Remote Sens.* **57**, 1256–1264 (2019).
191. Bull, D. L. et al. Arctic coastal erosion: modeling and experimentation (Sandia National Laboratories, 2020).
192. Islam, M. A., Lubbad, R. & Afzal, M. S. A probabilistic model of coastal bluff-top erosion in high latitudes due to thermoabrasion: a case study from Baydaratskaya Bay in the Kara Sea. *J. Mar. Sci. Eng.* **8**, 169 (2020).
193. Thomas, M. A. et al. Geometric and material variability influences stress states relevant to coastal permafrost bluff failure. *Front. Earth Sci.* **8**, 143 (2020).
194. Casas-Prat, M., Wang, X. L. & Swart, N. CMIP5-based global wave climate projections including the entire Arctic Ocean. *Ocean Model.* **123**, 66–85 (2018).
195. Liu, Q., Babanin, A. V., Zieger, S., Young, I. R. & Guan, C. Wind and wave climate in the Arctic Ocean as observed by altimeters. *J. Clim.* **29**, 7957–7975 (2016).
196. Ribal, A. & Young, I. R. 33 years of globally calibrated wave height and wind speed data based on altimeter observations. *Sci. Data* **6**, 77 (2019).
197. Dodet, G. et al. The Sea State CCI dataset v1: towards a sea state climate data record based on satellite observations. *Earth Syst. Sci. Data* **12**, 1929–1951 (2020).
198. Irgang, C. et al. Towards neural Earth system modelling by integrating artificial intelligence in Earth system science. *Nat. Mach. Intell.* **3**, 667–674 (2021).

Acknowledgements

A.M.I., P.P.O. and H.L. were supported by EU Horizon 2020 Nunataryuk project (grant number 773421). M.B. would like to acknowledge financial support from the Carlsberg Foundation (grant number CF20-0129). L.M.F. was supported by the US National Science Foundation (grant numbers 1927553 and 1927708). The work of A.V.B. was funded by the Russian Foundation for Basic Research (RFBR) (grant number 20-35-70002). S.A.O. was supported by the RFBR (grant number 18-05-60300). B.M.J. was supported by a grant from the US National Science Foundation (grant number OISE-1927553) and the Interdisciplinary Research for Arctic Coastal Environments (InteRFACE) project through the US Department of Energy. The authors thank A. Nereson (USGS) for developing Fig. 2 and Y. Nowak for developing Figs 4, 5.

Author contributions

B.M.J. was instrumental in initiating this paper. A.M.I. led the Review and organized the collaboration. All co-authors provided input on the manuscript text, figures and discussion of scientific content. In particular, L.M.F. drafted the Geodiversity of Arctic coasts section, A.V.B. and S.A.O. drafted the Drivers of Arctic coastal dynamics section, M.B. drafted the Climate sensitivity of Arctic coasts section, A.M.I. drafted the Arctic shoreline changes section, P.P.O. and H.L. drafted the Impacts of Arctic coastal erosion section and L.H.E. drafted Box 1. B.M.J. contributed to editing the paper. The work of A.M.I., M.B., L.M.F., A.E.G. and L.H.E. brought the paper to its final form.

Competing interests

The authors declare no competing interests.

Peer review information

Nature Reviews Earth & Environment thanks M. Lim, M. Strzelecki, J. Overbeck and the other, anonymous, reviewer(s) for their contribution to the peer review of this work.

Publisher's note

Springer Nature remains neutral with regard to jurisdictional claims in published maps and institutional affiliations.

© Springer Nature Limited 2022